

March 2019

Attachable Arm Bike for Alternative Wheelchair Propulsion

Caraline R. Wood

Worcester Polytechnic Institute

Erin Ann McCann

Worcester Polytechnic Institute

Heather Lynn Bourassa

Worcester Polytechnic Institute

Kylie M. Juarez

Worcester Polytechnic Institute

Zoe Schwartz

Worcester Polytechnic Institute

Follow this and additional works at: <https://digitalcommons.wpi.edu/mqp-all>

Repository Citation

Wood, C. R., McCann, E. A., Bourassa, H. L., Juarez, K. M., & Schwartz, Z. (2019). *Attachable Arm Bike for Alternative Wheelchair Propulsion*. Retrieved from <https://digitalcommons.wpi.edu/mqp-all/6712>

This Unrestricted is brought to you for free and open access by the Major Qualifying Projects at Digital WPI. It has been accepted for inclusion in Major Qualifying Projects (All Years) by an authorized administrator of Digital WPI. For more information, please contact digitalwpi@wpi.edu.



Attachable Arm Bike for Alternative Wheelchair Propulsion

A Major Qualifying Project Report submitted to the Faculty of the
WORCESTER POLYTECHNIC INSTITUTE
in partial fulfillment of the requirements for the Degree of Bachelor of Science

Submitted By:

Heather Bourassa

Kylie Juarez

Erin McCann

Zoe Schwartz

Caraline Wood

March 22, 2019

Submitted To:

Professor Brian J. Savilonis
Department of Mechanical Engineering

Table of Contents

Table of Contents	2
Table of Figures.....	4
Table of Tables	6
Acknowledgements	7
Abstract.....	7
Chapter 1: Introduction	8
Chapter 2: Literature Review	10
2.1 Overview of Wheelchair Users.....	10
2.2 Wheelchair Basics	10
2.3 Classic Wheelchair Propulsion Methods	12
2.3.1 Hand Rim Propulsion	12
2.3.2 Hub Crank Propulsion.....	13
2.3.3 Crank and Lever Propulsion	14
2.3.4 Hand Cycle Propulsion	15
2.4 Design Selection	16
2.5 Wheel Chair Attachments Currently on Market.....	17
2.6 Bicycle Mechanics	18
2.6.1 Upright Bicycle Composition	18
2.6.2 Chainless Drive Bicycles	19
Chapter 3: Design	20
3.1 Project Goal	20
3.2 Target Audience	20
3.3 Project Logistics	20
3.3.1 Project Timeline	20
3.4 Design Criteria	21
3.5 Engineering Design Standards.....	21
3.6 Design Evolution	22
3.7 CAD Model Designs	25
3.8 Final Design	27
3.8.1 Final Design of Hand Cycle	27
3.8.2 Final Design of Attachment to Wheelchair.....	27
3.9 Design Calculations	29
3.9.1 Gear Calculations	29
3.9.2 Stress Analysis (FEA)	31

Chapter 4: Prototype	40
4.1 Final Bill of Materials	40
4.2 Bike Construction	41
4.3 Attachment Mechanism Construction	43
Chapter 5: Prototype Field Testing	46
Chapter 6: Design Validation	49
Chapter 7: Recommendations and Redesign	52
7.1 Propulsion System	52
7.2 Hand Crank	56
7.3 Brakes	56
7.4 Steering	57
7.5 Frame	57
7.6 Attachability	58
7.7 Redesign Bill of Materials	59
Chapter 8: Conclusions	61
Chapter 9: References	62
Chapter 10: Appendices	64
Appendix A: Part Models and Drawings Prototype	64
Two Inch PVC Pipe	64
Two Inch Elbow	65
Two Inch T Connector	66
$\frac{3}{4}$ Inch Pipe	67
$\frac{3}{4}$ Inch Elbow	68
$\frac{3}{4}$ Inch T Connector	69
$\frac{3}{4}$ Inch Wye Connector	70
Bevel Gear	71
Bevel Pinion Gear	72
Miter Gear	73
Shoulder Bolt	74
Bearing (Shaft)	75
Bearing (Axle).....	76
Spacer for Fitting (Crank)	77
Spacer for Two-Inch PVC Pipe	78
Spacer for Fitting (Shaft)	79
Metal Clip	80
Metal Wheelchair Attachment Points	81
Appendix B: Assembly Drawings Prototype	82
Appendix C: Gear Calculations Prototype	83

Table of Figures

Figure 1: Classic Hand Rim Propelled Wheelchair [4].....	8
Figure 2: Variety of Powered and Mechanical Wheelchairs [10].....	11
Figure 3: Manual Wheelchair Components [11].....	11
Figure 4: Applied Force and Muscle Usage Directions [14]	12
Figure 5: a) Effective Force Direction b) Actual Force Direction Sketch c) Kinematics Diagram [16]	13
Figure 6: Example Hub Crank [15].....	13
Figure 7: Drive Mechanism of a Lever Propelled Wheelchair [18]	14
Figure 8: Kinematics of Lever Propulsion Diagram [13]	15
Figure 9: Kinematics of Hand Cycle Propulsion [20].....	16
Figure 10: Comparison of Different Propulsion Mechanisms [17]	17
Figure 11: Bicycle Component Diagram [24].....	18
Figure 12: Belt Drive System [26]	19
Figure 13: Drive Shaft Drivetrain [25]	19
Figure 14: Gantt Chart of Project Timeline	21
Figure 15: Functional Goals Design Matrix	22
Figure 16: Drive Shaft Concepts [25]	23
Figure 17: Sketch of Hand Crank	23
Figure 18: Initial Attachment Mechanism Design [27]	24
Figure 19: Final Sketch of Arm Bike Preliminary Design.....	24
Figure 20: Rank Order Design Matrix	25
Figure 21: First CAD Design - Non-Symmetrical	25
Figure 22: Second CAD Design Symmetrical - Six-Inch Elbows	26
Figure 23: Third CAD Design - Asymmetrical Six-Inch Elbows.....	26
Figure 24: Isometric and Front View of Final Hand Cycle CAD Design.....	27
Figure 25: Steering Mechanism CAD Model	28
Figure 26: Attachment Framework CAD Model	28
Figure 27: Free Body Diagram of System	30
Figure 28: FEA Mesh Crankshaft	31
Figure 29: Split Dimensions of Crankshaft.....	31
Figure 30: Loads Applied for Crankshaft FEA.....	32
Figure 31: Crank Shaft Stress Analysis Results.....	32
Figure 32: FEA Mesh Drive Shaft	33
Figure 33: Split Dimensions of Drive Shaft.....	33
Figure 34: Loads Applied for Drive Shaft FEA.....	34
Figure 35: (L) Drive Shaft Stress Analysis Results; (R) Bottom View Shaft Stress Results	34
Figure 36: FEA Mesh Bevel Gear.....	35
Figure 37: Loads Location Drawing Bevel Gear	35
Figure 38: Bevel Gear Stress Analysis Results.....	36
Figure 39: FEA Mesh Pinion Gear	36
Figure 40: Loads Location Drawing Pinion Gear	37
Figure 41: Pinion Gear Stress Analysis Results.....	37
Figure 42: FEA Mesh Miter Gear	38
Figure 43: Loads Location Drawing Miter Gear	38
Figure 44: Miter Gear Stress Analysis Results	39
Figure 45: Preparing the Wheel	41
Figure 46: Frame Subassembly Drawing and BOM.....	42

Figure 47: Crank Configuration	43
Figure 48: Crank Connection to Bike	43
Figure 49: Steering Hitch	44
Figure 50: Wye Connector Secured to Wheelchair	44
Figure 51: Configuration of PVC Connection	44
Figure 52: Complete Prototype Assembly	45
Figure 54: Turning Radius Diagram	46
Figure 54: Photos from Testing the Prototype	47
Figure 55: Right Angle Speed Reducer [28]	53
Figure 56: Inline Planetary Speed Reducer [28]	53
Figure 57: Engineering Drawing of Parallel Speed Reducer [28]	53
Figure 58: Redesign Propulsion System Schematic	54
Figure 59: Output Redesign Shaft and Drawing [28]	54
Figure 60: Input Redesign Step Shaft [28]	55
Figure 61: Shaft Coupling Figure and Drawing [28]	55
Figure 62: Shaft Ball Bearings Redesign [28]	55
Figure 63: Wheel and Axle Redesign [28]	56
Figure 64: Hand Crank Sketch Redesign	56
Figure 65: Brakes Redesign [22]	56
Figure 66: Rio Dragonfly Chain Drive with Telescoping Feature [22]	57
Figure 67: Frame Tubing Redesign [28]	57
Figure 68: Dragon Plate Telescoping Tube Clamp [20]	57
Figure 69: Dragonfly Handcycle Attachment Mechanism [27]	58
Figure 70: Location of Ball Clamps on Wheelchair Frame [27]	58
Figure 71: Ball Clamp Parts [27]	58
Figure 72: Location of Bottom and Top Links and Couplers [27]	58
Figure 73: Two Inch PVC Pipe Engineering Drawing [28]	64
Figure 74: Two Inch PVC Elbow Engineering Drawing [28]	65
Figure 75: Two Inch PVC Tee Connector Engineering Drawing [28]	66
Figure 76: 3/4 Inch PVC Pipe Engineering Drawing [28]	67
Figure 77: 3/4 Inch PVC Elbow Connector Engineering Drawing [28]	68
Figure 78: 3/4 Inch PVC Tee Connector Engineering Drawing [28]	69
Figure 79: 3/4 Inch PVC Wye Connector Engineering Drawing [28]	70
Figure 80: Bevel Gear Engineering Drawing [28]	71
Figure 81: Bevel Pinion Gear Engineering Drawing [28]	72
Figure 82: Miter Gear Engineering Drawing [28]	73
Figure 83: Shoulder Bolt Engineering Drawing [28]	74
Figure 84: 0.75-Inch Shaft Diameter Ball Bearing Engineering Drawing [28]	75
Figure 85: Ten Millimeter Shaft Diameter Ball Bearing Engineering Drawing [28]	76
Figure 86: Spacer for Crank Shaft in 3/4-Inch PVC Fitting Engineering Drawing	77
Figure 87: Spacer for Shaft Bearing in Two-Inch PVC Pipe Engineering Drawing	78
Figure 88: Spacer for Shaft Bearing in Two-Inch PVC Fitting Engineering Drawing	79
Figure 89: Metal Clip for Attachment Engineering Drawing [28]	80
Figure 90: Adjustable Angle Steel Clamp Engineering Drawing [28]	81
Figure 91: Hitch Assembly Engineering Drawing	82

Table of Tables

Table 1: Comparison of alternative propulsion attachments currently on the market [H18-H20]	18
Table 2: Weights of Components in System.....	29
Table 3: FEA Loads Crankshaft.....	32
Table 4: FEA Results Crank Shaft	33
Table 5: FEA Loads Drive Shaft.....	34
Table 6: FEA Results Drive Shaft.....	34
Table 7: FEA Loads Bevel Gear	35
Table 8: FEA Results Bevel Gear	36
Table 9: FEA Loads Bevel Gear	37
Table 10: FEA Results Pinion Gear	38
Table 11: FEA Loads Miter Gear	39
Table 12: FEA Results Miter Gear	39
Table 13: Raw Data from Testing on Bartlett Ramp	47
Table 14: Raw Data from Testing on Quad	47
Table 15: Redesign Bill of Materials	60

Acknowledgements

We would like to thank the following people and organizations for their contributions to this project.

- Professor Brian Sivilonis for his guidance and input throughout all stages of this project.
- Worcester Earn-A-Bike and Patrick Goguen for his insight on bike manufacturing and design.
- Spaulding Rehabilitation Hospital representatives for their advice on design constraints and product needs.
- WPI Office of Disability Services and Jessica Szivos for her background knowledge on the project's target audience and similar existing products.

Abstract

Current options for alternative wheelchair propulsion devices are cumbersome, expensive, and dangerous if transfer from wheelchair to another device is required. Devices with chains are unreliable due to chain breakage or derailment. To combat these shortcomings, this project created a gear and drive shaft powered, attachable arm bike prototype. This project validates the concept of a chainless arm bike and lays the groundwork for future products that are more compact and less expensive than existing models.

Chapter 1: Introduction

Mobility is an essential part of many people's lives, but its importance is often taken for granted until it is hindered either temporarily or permanently. At the present time, approximately 132,000,000, or 1.85% of people in the world cannot walk long distances on their own, and therefore require a wheelchair or assistive mobile device for movement. With the world's population increasing daily, the need for wheelchairs expands by about 3,500 wheelchairs every day. Of these millions of wheelchairs being used globally, about 90% are hand rim propelled, thus dominating the market [1]. Hand rim propulsion is the classic style of wheelchair propulsion where the individual reaches back, grasps a set of rims attached to the wheels, and pulls forward. Although this mode of propulsion is the most common, it has been proven to be inefficient and harmful to individual's musculoskeletal and cardiopulmonary systems over time due to upper body overuse [2]. This is a result of the repetitive motion and mechanical labor necessary to propel this style of wheelchair forward. Studies have shown that people who are confined to a wheelchair over a long period of time are prone to developing upper body injuries, mostly in the hand and shoulder areas [3]. In efforts to mitigate these injuries and to improve the motion of wheelchairs, research has been done to develop alternative wheelchair propulsion methods that cause less stress on the body while keeping individuals active and healthy.



Figure 1: Classic Hand Rim Propelled Wheelchair [4]

Alternative options currently on the market for hand rim propulsion include a variety of both motorized and mechanical solutions. The motorized units typically have an external power source, such as motor, that propels the wheelchair forward when the user prompts through a remote or other electric control system. The mechanical solutions are typically wheelchairs or wheelchair attachments that still require energy expended by the user to create motion, however this energy is inputted through a different motion than the classic hand rim propelled movement. Common mechanical motions for propulsion include hand cycling, cranks, and lever systems which all produce the same wheelchair movement with less upper body strain.

For this project, the team developed a prototype that mitigates upper body strain, increases mechanical efficiency, and improves the overall experience of wheelchairs users during locomotion. For this purpose, the team researched current alternative propulsion methods to determine their shortcomings through user testimonials and published literature. Ultimately the team concluded that individuals using standard hand rim propelled wheelchairs are inherently at risk of health complications such as upper extremity strain and cardiovascular disease as a result of inactivity. Current options for alternative propulsion devices can be cumbersome, expensive, and dangerous if transfer is required. They have also been shown to be unreliable in cases where chains are involved due to chain breakage or derailment. To combat these shortcomings, this project aimed to prototype an adjustable, portable, and chainless driven hand cycle that would easily attach to standard hand rim propelled wheelchairs. This device will ideally mitigate muscular strain, promote physical activity, and improve wheelchair user's experiences.

Chapter 2: Literature Review

2.1 Overview of Wheelchair Users

Approximately 65 million people in the world have disabilities that lead to mobility impairment and the need for assistive technologies for transportation [5]. Common causes for mobility impairment include amputation, spinal cord injury, cerebral palsy, paralysis, multiple sclerosis, muscular dystrophy, and other orthopedic or neurological disorders [6]. The extent of the functional abilities of these individuals fluctuates drastically on the global scale and varies from complete paralysis to near full functionality. Factors influencing the performance level of these individuals include the severity of their disorder, their access to healthcare, as well as the culture and lifestyle they live in [6]. Due to the extensive variability of functionality among individuals with mobility impairments, this project will specifically focus on serving paraplegics.

Paraplegics, those with motor and or sensory impairments in the lower extremities, almost exclusively consist of individuals who have experienced damage to the brain and or spinal cord as a result of a traumatic injury [7]. When such damage occurs, the communication link between the brain and the lower region of the body is lost, which results in a loss of both motion and sensation [7]. Studies have also shown that individuals with paraplegia have lower levels of physical exertion and respiratory function, as well as lower maximum heart rates when compared to fully functioning individuals. Paraplegics, specifically those with spinal cord injuries (SCI), are not capable of independent mobility and thus are not capable of the standard forms of physical activity and exercise the remainder of the population is accustomed to. Due to their decreased mobility and reduced function, they are at higher risk for obesity and other cardiovascular diseases [8]. For these individuals to avoid the risks associated with a sedentary lifestyle, those using wheelchairs are advised to seek out other forms of physical activity through upper body use [8].

To assist individuals with mobility impairments, assistive technologies of varying complexities have been developed to help promote ease of transportation. These solutions vary from simple devices with minimal technology, including canes, walkers, and manual wheelchairs, up to very complex and technologically advanced devices, such as modern powered wheelchairs that can orient an individual vertically and climb stairs [6]. Of the 65 million individuals who require assistive technology for mobility, 20 million go without the assistance they need and struggle daily due to their impairment [5].

2.2 Wheelchair Basics

The wheelchair is one of the most common assistive technologies used in the world to combat mobility impairments, followed closely by canes and walkers [5]. Wheelchairs are praised for their versatility, because they are customizable.

To accommodate the wide range of applications required for wheelchair use, there are several different styles used by disabled individuals. The two largest categories of wheelchairs are manual wheelchairs and powered wheelchairs. Manual wheelchairs are purely mechanical

and require no external power sources to function. Whereas power wheelchairs use motors powered by batteries. Power wheelchairs have the advantage of requiring minimal effort and low ranges of motion from the user, so more people can use the product. Alternatively, classic manual wheelchairs require close to, if not full functionality of the upper body for propulsion. Other advantages of power wheelchairs include their speed capabilities and potential for long distance travel without fatigue. There are several disadvantages that come with power wheelchairs, including cost, difficulty of navigation, and the sedentary lifestyle it promotes, which can lead to obesity and chronic heart problems. The manual wheelchair global market accounts for 2.9 billion dollars, and the power wheelchair market accounts for 3.9 million dollars [9]. With an aging global population, the revenue from this industry is expected to grow in the coming years at a predicted rate of 2.8% per year [9].



Figure 2: Variety of Powered and Mechanical Wheelchairs [10]

Manual wheelchairs come in many different variations, such as standard/everyday wheelchairs, youth wheelchairs, lightweight wheelchairs, reclining wheelchairs, sport wheelchairs and more. These wheelchairs can come in many different frames but are mainly comprised of the same basic components.



Figure 3: Manual Wheelchair Components [11]

2.3 Classic Wheelchair Propulsion Methods

For those who are restricted to wheelchairs due to lower body paralysis, the motions that can be used to generate an effective cardiovascular focused workout, while still propelling the wheelchair are severely restricted. For those with lower body monoplegia, hemiplegia, paraplegia, or quadriplegia, any exercise using legs, core, or lower back muscles are not feasible [12]. As such, motions for most wheelchair and wheelchair appendages focus on using muscles in arms, shoulders, and the upper back exclusively. Additionally, motions that produce the highest degree of cardio while mitigating chronic pain, strain, and effort because of repeated motion are favored. As such, in the following section several different motions are examined, each of which use only those muscles in the upper body to generate a cardio workout. Motions are assessed and analyzed based on biomechanics, cardiovascular and respiratory responses, and propensity for chronic strain and injury [12].

2.3.1 Hand Rim Propulsion

One simple way for an individual restricted to a wheelchair to get a cardiovascular workout is through classic wheelchair propulsion at high intensities. This motion uses the hands, arms, shoulders, and chest, consequently engaging the biceps, triceps, pectoral muscles, and deltoid muscles in the process [13]. Joints involved in classic wheelchair propulsion include the metacarpal joints, the carpal joint, the elbow joints, and the shoulder joints [14].

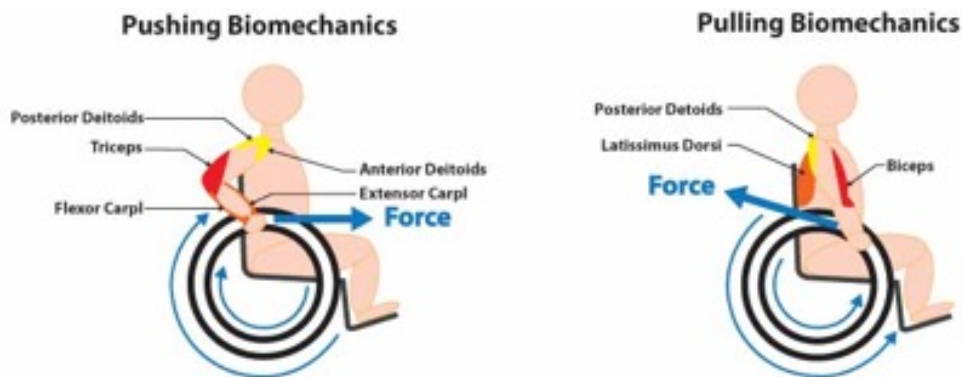


Figure 4: Applied Force and Muscle Usage Directions [14]

Extensive research has been completed to quantify the effectiveness of hand rim wheelchair movements. The typical propulsion cycle is broken into a working phase, when the force is applied, and a rest phase, when the arms release the wheel and return to their original position. One common critique of this method is the ratio of time spent working compared to resting. In a typical push of a wheelchair, the entire cycle takes approximately one second. Of this time, only 0.2-0.6 seconds is spent applying a force to the wheels [15]. This leads to a motion with a low mechanical efficiency, which through testing has been quantified to equal approximately 10% [15].

Beyond low efficiency, there is an added drawback of producing long-term strain and pain in individuals. When people propel themselves, they apply a force downwards and

forwards, as shown in Figure 5b. Only the component of the force tangential to the wheel, which is about 40% of the total propulsion torque, contributes to propelling the wheelchair, as shown in Figure 5c [16]. Due to the difference between the effective force angle and the actual force direction, the muscles and cardiopulmonary systems are significantly strained which can cause chronic pain [15]. Repetitive high force applications are believed to be major causes of carpal tunnel syndrome in wheelchair users [16]. In the shoulder joint, similar strains are produced which also lead to long term injuries and impairments.

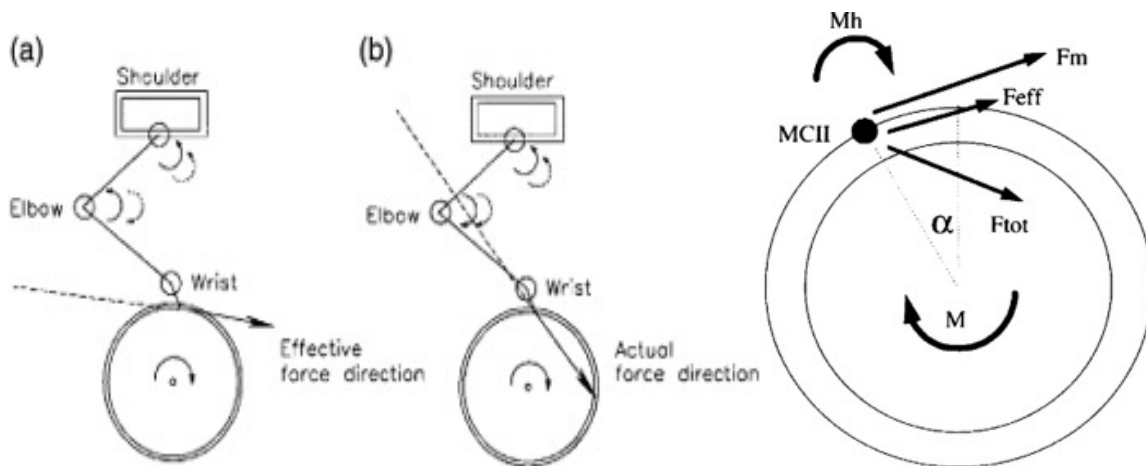


Figure 5: a) Effective Force Direction b) Actual Force Direction Sketch c) Kinematics Diagram [16]

2.3.2 Hub Crank Propulsion

One alternative propulsion method that is relatively unknown is the hub crank. This device, shown in Figure 6, consists of two cranks connected to the wheel hub that allow the hands to continuously move around the wheel hubs of a wheelchair. The use of hub cranks makes it so that steady force is exerted on the wheels, in a similar orientation as hand rim propulsion [17]. This alternative propulsion method is utilized mostly in racing and athletics, but it is not practical for everyday use due to the complicated steering and braking systems [17].



Figure 6: Example Hub Crank [15]

Although there are drawbacks relating to maneuverability, it has improved efficiencies and reduced strains when compared to traditional wheelchair propulsion. Studies show that the hub crank produces a gross mechanical efficiency of approximately 13 percent. This is about

three percent higher than the mechanical efficiency of traditional wheelchair propulsion [15]. The handgrip is designed to match the orientation of the hand, allowing a reduced counteracting hand moment during propulsion, which allows the effective force to be greater [15,16]. This natural hand position produces less strain in the wrist, allowing for a more pain free and comfortable experience [15].

2.3.3 Crank and Lever Propulsion

Crank and lever propulsion systems were popular alternative motions throughout the 1950s and 60s. These movements reduce strain on the body, compared to hand rim propulsion, but their large size and weight are major drawbacks [17]. In this method, the hands follow a cyclic motion in either a synchronous or asynchronous way, with lever mechanisms working in a perpendicular plane ventral to the user [17]. The force produced is transferred directly to the wheels through a simple push/pull lever device. One specific type of lever propulsion is the crank-to-rod mechanism. This commercially available lever design is a simpler, less energy consuming and more efficient type of propulsion. It consists of a simple lever propulsion system that drives the back wheels by a crank-and-rod mechanism fixed on the hub of the back wheels [17] as shown in Figure 7. This allows for higher velocities over longer durations resulting in lower strains on the body. The length of the levers can be adjusted and compared to hand rim, the hands are in a much more natural position [17].

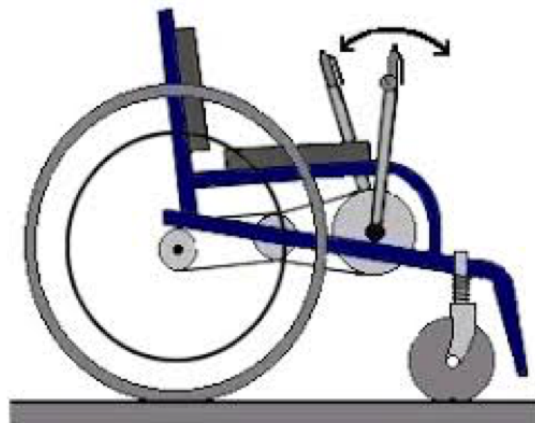


Figure 7: Drive Mechanism of a Lever Propelled Wheelchair [18]

The lever propelled system functions by applying a rotational force on a lever that is connected to the wheels of the wheelchair through a train of gears. Rather than reaching horizontally to rotate the wheels and propel forward, motion is generated through a push-pull mechanism in front of the body [15]. As a result, the mechanical efficiency of this motion is about 3 percent greater than the efficiency seen in the traditional hand crank motions [15]. The lever has the added benefit of employing both a push and pull motion in its cycle, engaging flexion and extension equally, unlike in rim propulsion where the push motion is heavily relied on. This consequently applies the total external force in the body closer to the center of the shoulder than in rim propulsion, reducing the torque in the shoulder and mitigating long term strain [15]. Of all the motions, the lever mechanism has the lowest, almost negligible, energy loss between the body and machine components [15].

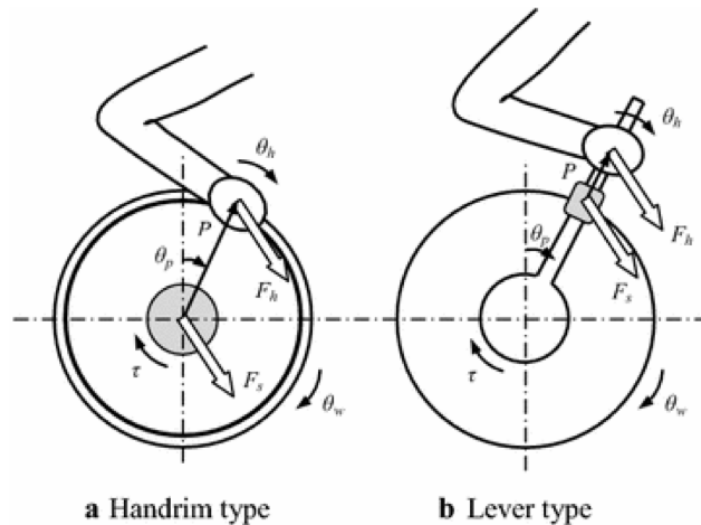


Figure 8: Kinematics of Lever Propulsion Diagram [13]

2.3.4 Hand Cycle Propulsion

Arm-crank propulsion, also known as hand biking or hand cycling, is an alternative wheelchair propulsion method that provides guided movement. Research shows that hand cycling is far more efficient than hand rim propulsion, producing an average mechanical efficiency of 16.3% versus hand rim's 11.6%. Additionally, the motion has a higher average power output than classic propulsion [15]. Hand cycling is a less strenuous and more efficient propulsion method than hand rim propulsion, with respect to efficiency and cardiorespiratory effects.

In hand cycling, the arms and hands work together to achieve power transfer and steering. Trunk movement is an important parameter to factor in when considering the ergonomics of a hand cycle. Based on the degree of a person's trunk functionality and abdominal strength, there are two propulsion types, arm-power and arm-trunk-power propulsion [17]. Hand cycles can have two different crank configurations, either synchronous or asynchronous. Synchronous involves the cranks in parallel positions, where asynchronous cranks are rotated 180 degrees from one another. Research shows that synchronous hand cycling is less strenuous and more efficient than asynchronous cycling [17].

The biomechanics of hand cycling revolve around crank angles from 0-360 degrees. The motion between 0-180 degrees is associated with the "pull" motion, where the biceps are activated, and elbows are in flexion [13]. This pull motion is where muscles, such as the deltoideus, trapezius and serratus anterior are activated and the highest forces are produced [13]. Between the 180-360-degree cycle, the triceps are engaged, the elbows are extended and a "push" motion is obtained. The distribution of forces throughout the propulsion cycle show that the greatest average external force is applied when pulling the crank (30-90 degrees) [19]. The highest force on the glenohumeral joint is produced during the pulling/lifting of the crank (0-270 degrees) due to muscles fighting gravity [19]. Throughout the propulsion system, the muscles that produce the highest amount of force are the deltoideus (scapular), triceps and trapezius [19].

Overall, research shows that during arm cycling, external forces can be distributed more evenly throughout the whole cycle, which results in less strain than hand rim propulsion [19].

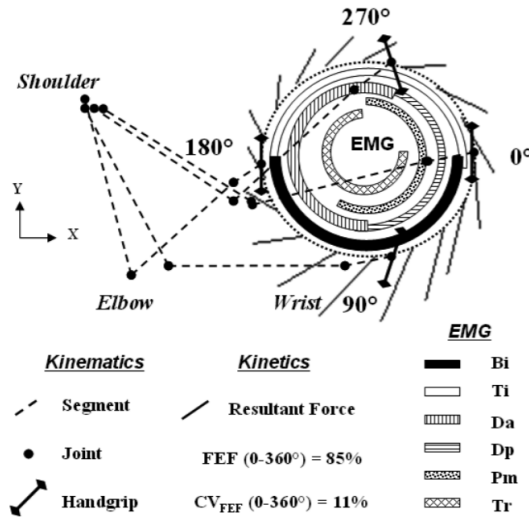


Figure 9: Kinematics of Hand Cycle Propulsion [20]

2.4 Design Selection

There are a number of alternative propulsion methods that mitigate the muscular strain applied to the body while providing efficient wheelchair locomotion. In the design and prototype stage, the team elected to focus on one singular propulsion motion to optimize. Early in the design process, the team chose between hand cycle, crank and lever, and hub crank motions. Of these three types of wheelchair propulsion, the team chose a motion that would mitigate muscular strain, maximize work efficiency, and provide an enjoyable and intuitive user experience. Using the table shown below, it was determined that an attached hand cycle would be best for the purposes of this project. Of the three methods, handcycle and lever motions produced the highest mechanical efficiencies and lower muscle strains, while producing similar maximum speeds [17]. The deciding factor between the two motions was portability and maneuverability. This study ranked the attachable hand cycle unit superior for both outdoor use and transportation. For these reasons the hand cycle motion was selected for use in this project.

TABLE 1
Characteristics of different propulsion mechanisms, partly based on experimental data



	Hand Rim		Hand Cycle			
	Basket	Racing	Fixed	Attach Unit	Lever	Hub
Max ME (%)	<10	<8	>13	>13	>13	>12
Strain CVS	High	High	Low	Low	Low	Low?
Strain MSS	High	High	Low	Low	Low	Low?
Risk RSI	High	High	Low?	Low?	Low?	Low?
Top speed (km · hr ⁻¹)	15	30	>30	30	30	30
Mass (kg)	<10	<8	10	15	10	<10
Coupling hand	-	-	++	++	++	+
Force direction	-	-	+	+	++	+
Bimodal	-	+	+	+	+	+
Continuous work production	-	+	+	+	+	+
Outdoor use	+	++	+++	+++	++	+
Maneuverability	++	±	-	-	-	-
Indoor use	++	±	-	±	-	-
Steering	++	±	±	±	±	-
Brake	±	-	+	+	+	-
Transportation	++	++	-	+	-	±
Maintenance	+	+	±	±	±	+

CVS, cardiovascular system; MSS, musculoskeletal system; RSI, repetitive strain injury.

Figure 10: Comparison of Different Propulsion Mechanisms [17]

2.5 Wheel Chair Attachments Currently on Market

Most commercially available alternative propulsion methods are expensive and are not covered by classic health insurances. Additionally, many products are large, heavy, and cumbersome, making indoor navigation difficult. In the table below, three popular wheelchair attachments are compared to introduce the wheelchair accessory market and identify the unmet needs of the customer at the present time.

Name	Company	Image	Description	Price	Weight	Pros	Cons
Dragonfly [21]	Rio Mobility		Synchronous Hand Cycle Propelled with Chain	\$1800	21.5 lbs.	User gets a cardiovascular and upper body workout with minimal chronic strain	Chain derailment can be a major issue
Firefly [22]	Rio Mobility		Battery Powered Electric Attachment. 350 W Motor. 4 Hour Battery Life	\$2400	24 lbs.	Capable of traveling long distances due to minimal fatigue	User gets minimal exercise putting them at risk of obesity and heart disease

<p>Wijit Wheelchair Lever Driving and Braking System [23]</p>	<p>Wijit</p>		<p>Lever System where user pushes forward to propel</p>	<p>\$4500</p>	<p>10 lbs.</p>	<ul style="list-style-type: none"> - Compact Design - Requires ½ the effort of hand rim propulsion - Protects hands from elements/tires 	<ul style="list-style-type: none"> -Backwards propulsion not possible - Lever motion only allows for asynchronous motion
---	--------------	---	---	---------------	----------------	--	--

Table 1: Comparison of alternative propulsion attachments currently on the market [21-23]

2.6 Bicycle Mechanics

2.6.1 Upright Bicycle Composition

Two-wheeled upright bicycles are fabricated from numerous parts. The frame of the bicycle is composed of a top tube, down tube, seat tube, and seat stay, as seen in Figure 11. The frame is the main chassis for the bike, usually made of welded steel or aluminum. In most cases bicycles have a cable break system, mounted to the handlebars [24].

To propel the bicycle, foot pedals are connected to gears, a chain, chain ring, cassette, and derailleurs. The chain is composed of metal interlocking links and transmits energy from the pedals to the wheels. Derailleurs move the chain from one gear to the next, changing the speed of the bicycle. Gear shifts are mounted on the handlebars and are connected to the derailleurs and give the rider the ability to manually change their torque and speeds [24].

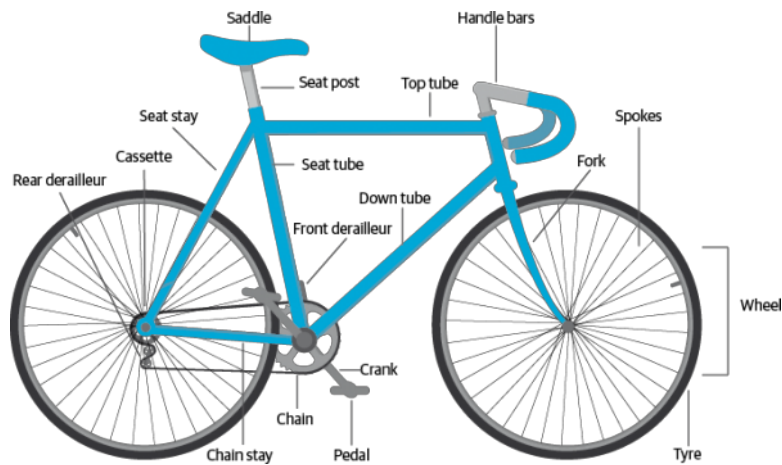


Figure 11: Bicycle Component Diagram [24]

An important aspect of a bicycle is the tube-in-tube steering system. A rotational motion of the handlebars must transfer the bicycles forward momentum in different direction. When the rider turns, the bicycle remains balanced because of the hinged connection between the rear frame and the front fork of the frame. Therefore, a steering mechanism that allows the user to remain vertical is crucial for the proper function of a bike and the safety of the rider.

2.6.2 Chainless Drive Bicycles

In many bicycles, the drive train system is a chain connected from the pedals to the wheels that transfers the mechanical energy to propel the bicycle forward [25]. Chains are an affordable, reliable and an easy to fix method of transmitting energy. Chains are also an extremely efficient way to transmit this energy: some reports indicate that the chain power transmission system is 98 percent efficient. A drawback of chains is that they frequently fall off the cassette and chain ring, which requires the rider to disembark from the saddle to replace the chain onto the cassette [25]. A chain system also requires maintenance to extend its life, such as lubrication; therefore, chainless drive systems are a design advantage in terms of portability and less frequent maintenance [25].

An alternative to a chain drive bicycle is a belt drive system. An advantage to the belt drive system is that it requires no maintenance. However, some belt drive systems on the market do not have sprockets to hold the belt in place, which causes it to slip and significantly reduces the mechanical efficiency [26]. A disadvantage of this drive system is that it does not have a derailleur meaning it is a single speed system. Also, a broken belt cannot be fixed so the rider would have to change the belt entirely if it broke meaning a spare belt would always have to be carried around [26].



Figure 12: Belt Drive System [26]

Another alternative to chain and belt drive mechanisms is a drive shaft. This drive system uses a series of pinion and beveled gears and a shaft to transmit power from the pedals to the wheels, propelling the rider forward. This drive system reduces the number of friction contact points and in turn increases the mechanical efficiency. A prototype of this mechanism called the Ceramic Speed chainless drive train (shown below) states that an output of 380 watts of power increases the efficiency of the bicycle to 99% [25].



Figure 13: Drive Shaft Drivetrain [25]

Chapter 3: Design

3.1 Project Goal

The goal of this project was to design and prototype a functional, adjustable, and chainless hand cycle that easily attaches to standard hand rim propelled wheelchairs and mitigates muscular strain, promotes physical activity, and improves the wheelchair user's experience. This device was intended to be intuitive, customizable to support user exercise preferences, and less expensive than current products on the market.

3.2 Target Audience

The target audience for this device was wheelchair users with full use of their upper extremities who were looking for alternative means of exercise and locomotion. Users must have full range of motion in their shoulders, elbows, wrists, and hands, and should have enough grip strength and arm power to pedal a classic arm bike. They must own a standard manual wheelchair that has no added power features.

3.3 Project Logistics

As this project is an academic venture funded by the university, there were several time and monetary restraints that the project team had to operate within. The following section outlines the project timeline and the project budget that the team adhered to.

3.3.1 Project Timeline

This project followed a classic algorithmic design process that consisted of a needs assessment, a design phase, and an iterative prototyping process, all of which were completed between the months of August and April. As highlighted in the Gantt chart, A-term was reserved for background research and preliminary design creation. The early stages of building began in B-term, beginning with small-scale models to display ideas, working up to the large-scale prototype for testing. By the end of B-term the team built a functioning drive shaft and frame. In C-term the team refined the prototype to improve functionality, and an attachment mechanism was designed, constructed, and installed. In the early weeks of D term, the team tested the device, made alterations as necessary, and finalized the calculations and documentation.

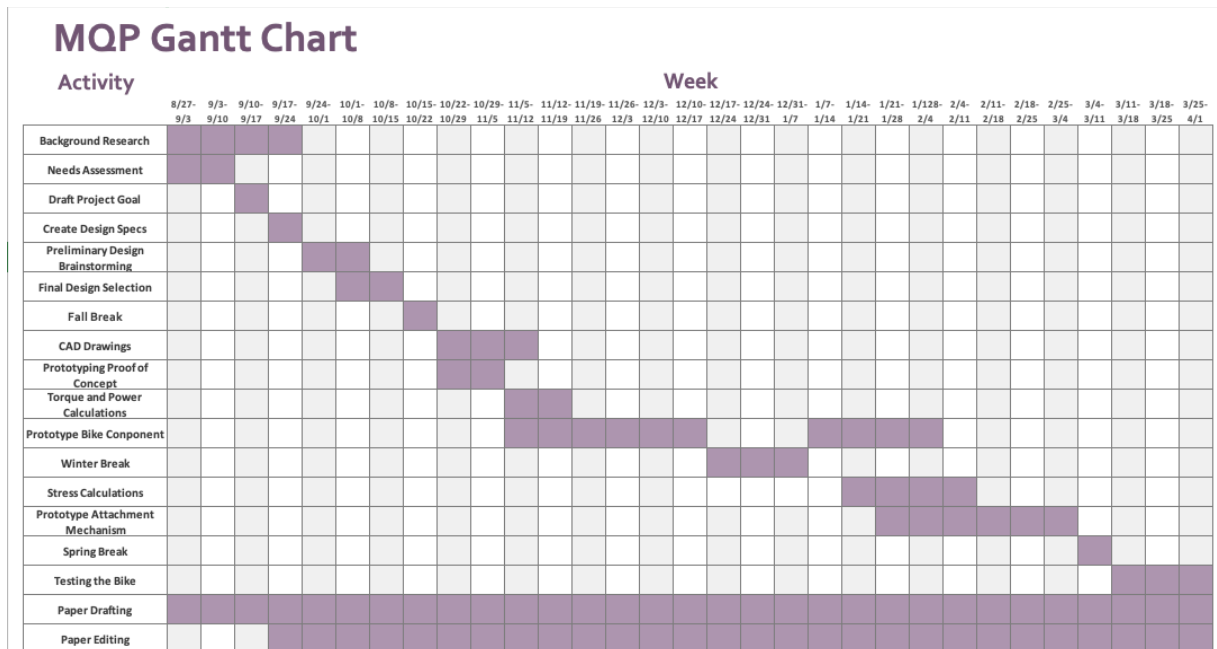


Figure 14: Gantt Chart of Project Timeline

3.4 Design Criteria

With the project goal in mind, there are several key design requirements and performance specifications that the team considered to create a desirable product for wheelchair users. These criteria were developed using current marketplace product reviews, clinical professionals' input, and technical literature on the topic. The team selected the following design objectives as the most crucial to the project goal.

1. Bike can be attached to most standard manual propulsion wheelchairs.
2. Bike avoids the use of chains, which are known for the propensity for derailment.
3. Bike can last for a minimum of five years.
4. Bike costs less to than \$750 manufacture.
5. Bike can start from rest with less than or equal to five pounds of input crank force.
6. Bike can travel at least at two m/s.
7. Bike weighs less than 20 lbs.
8. Bike has a 1-2-meter turn radius.
9. Bike can brake and safely stop within 2 meters.
10. Bike is portable and collapsible.

3.5 Engineering Design Standards

There are extensive regulations and standards for wheelchair and wheelchair accessory design intended to optimize the safety and enjoyment of the user. Since the prototype is a passive device, none of the electric regulations apply; however, there are standards for manual wheelchairs that the finalized device must adhere to. All standards for commercial wheelchairs are found in the ISO 7176 1-30 and 16840 1-12 standards. These standards discuss regulations

regarding the static stability, the dimensions, strength, and brake effectiveness. Since this is a prototype it will likely not meet all the above requirements [H21].

3.6 Design Evolution

This section details the process the team used to create, analyze, and eliminate preliminary design ideas to develop the final design. Based on the needs assessment and design specifications created, the team generated preliminary designs for the arm bike. The team broke the bike down into six systems: propulsion, steering, braking, attachability, hand crank, and frame. The team generated ideas for each aspect using circle sketches, which allows for independent idea generation and collaboration. Once this process was complete, the team grouped similar ideas together and discussed until several unique and different ideas were brainstormed. These ideas are shown below in the functional goals design matrix. After idea generation, the team discussed the merits and drawbacks of each idea and selected the option from each bike aspect category that would best adhere to the design requirements.

Propulsion	Chain	Drive shaft with gears	String chain	Belt drive	Meshed gears in casing
Steering	Tube in Tube				
Braking	Backwards Brake	Hand Brake			
Hand Crank	Asynchronous	Synchronous	Asynchronous and Synchronous		
Attachability	Two point attachment	Pin attachment	Clamps		
Frame	One piece	Collapsible Detachable	Foldable		

Figure 15: Functional Goals Design Matrix

Ideas for the propulsion of the device included metal chain, gear driven drive shaft, string chain, belt drive, and meshed gears in a casing. Ultimately the team elected to use a drive shaft with gears, as this appeared to be the most durable and realistic option. Team members raised concerns regarding if the materials of belt and string systems could withstand repeated loadings over extended periods of time. The meshed gears in a casing approach was too bulky and cumbersome, and the chain approach had too high of a risk of derailment. A sketch and a photo highlighting the key ideas of the selected drive shaft proposal are shown below.

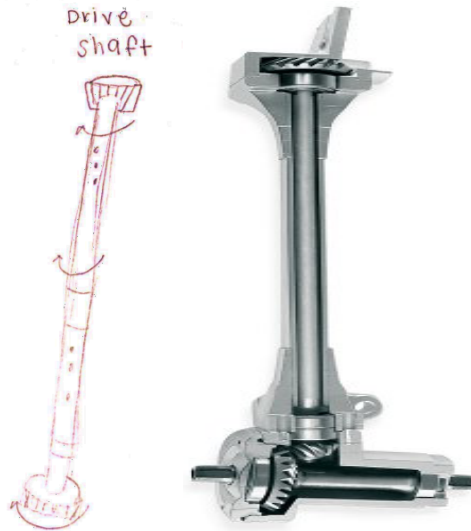


Figure 16: Drive Shaft Concepts [25]

For the hand crank the team considered three main options: a synchronous, an asynchronous, and a combination design. To appeal to a larger audience, the team chose a design that had both options available.

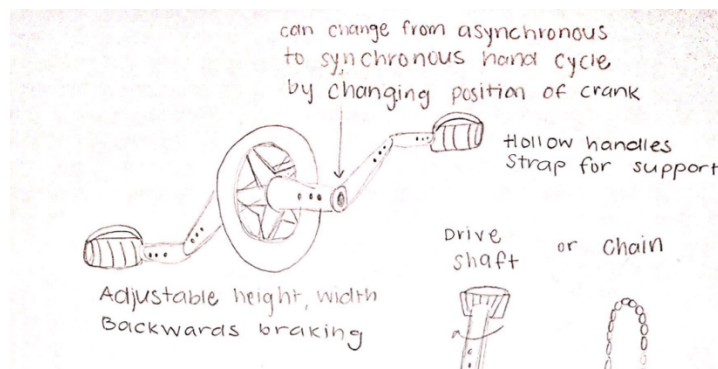


Figure 17: Sketch of Hand Crank

For the attachability mechanism, the team wanted to safely stabilize and secure the bike to the wheelchair while allowing for smooth steering. The team brainstormed a two-point attachment mechanism, a pin mechanism, and a clamp mechanism. In order to maximize stability and the weight bearing capabilities of the attachment piece, the team chose the two-point attachment design, as shown below, as it offers four total points of contact between the bike and the wheelchair.

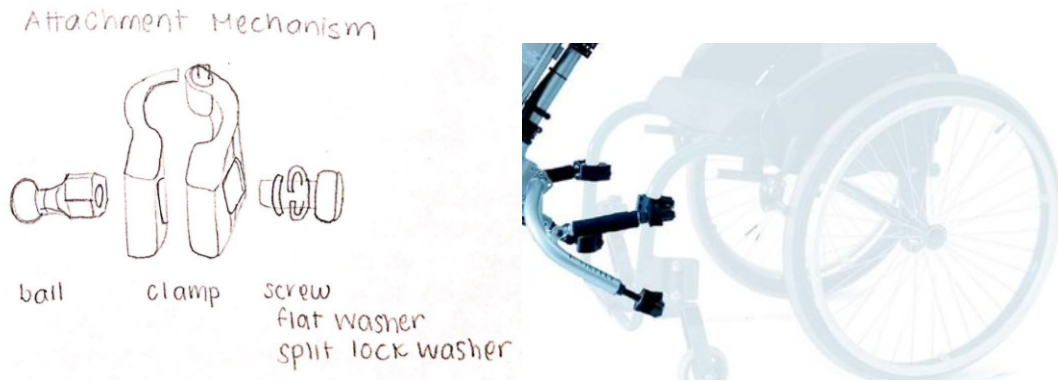


Figure 18: Initial Attachment Mechanism Design [27]

For the frame, the team discussed a solid frame made of one part, a collapsible frame, and a foldable frame. Of these options, the team chose the collapsible frame idea, as this promoted portability and was the most technically feasible of the three. A sketch combining all the selected elements into one preliminary design is shown below.

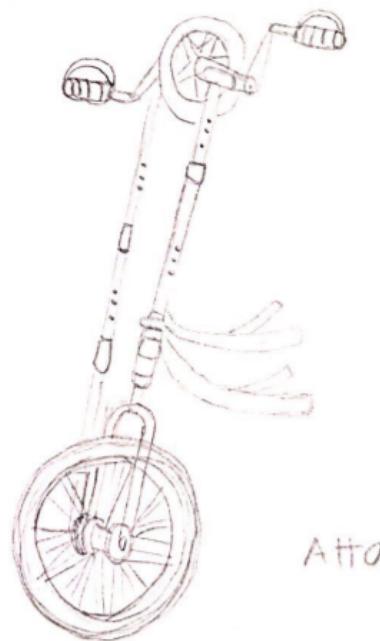


Figure 19: Final Sketch of Arm Bike Preliminary Design

Once the team selected and sketched designs, they prioritized which elements were the most important to the outcome of the project. The team used a rank order design matrix, where elements were compared to each other and given a 1, 0, or 1/2. A zero indicates the row is more important than the column, a 1/2 indicates they are equally important, and a one indicates the column is more important than the row. The rank order design matrix is shown below.

Rank order design matrix
 +Rank-Ordering Design Goals: 0(<), ½(=), 1(>) Read as column is ___ than row. Highest number has highest priority.
 Innovation aka New Design

	Attachability	Propulsion Mechanism	Wheels	Hand crank	Brakes	Steering	Frame
Attachability		1	0	1	0	0	0
Propulsion Mechanism	0		0	1	0	0	0
Wheels	1	1		1	1/2	1/2	1
Hand Crank	0	0	0		0	0	0
Brakes	1	1	1/2	1		1/2	1
Steering	1	1	1/2	1	1/2		1
Frame	1	1	0	1	0	0	
Totals:	4	5	1	6	1	1	3

Figure 20: Rank Order Design Matrix

3.7 CAD Model Designs

Throughout the initial design phases, the team used SolidWorks modeling software to model different designs before prototyping. Each design was then analyzed and iterated until a final design with the necessary attributes was created. For ease of building, the prototype was made of PVC pipe and PVC fittings. The initial CAD design is shown below.

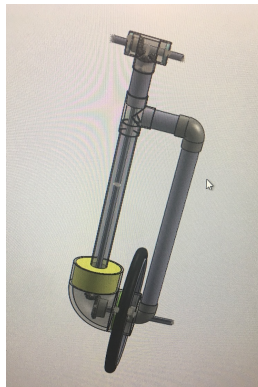


Figure 21: First CAD Design - Non-Symmetrical

An advantage of this design is that the crank handles can be close together. The shaft is stabilized using ball bearings press fit into spacers. This strategy of securing bearings using 3D printed spacers was used throughout the project. To house the gears on the left side, a six-inch PVC elbow and a large spacer were required. The size and weight of the six-inch elbow was not

feasible. This design was also not symmetrical which affected the center of gravity of the bike. For the next iteration the team decided to focus on making the bike symmetrical.

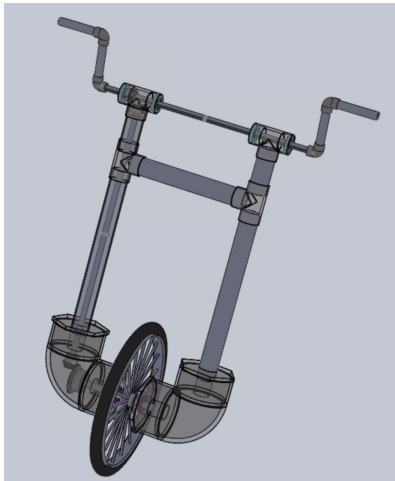


Figure 22: Second CAD Design Symmetrical - Six-Inch Elbows

This design features a symmetrical frame. The shaft is housed in two-inch PVC pipe and its respective fittings. Two six-inch elbows stabilize the bottom of the frame and the wheel axle. The drive shaft is stabilized within the PVC fittings with bearings and spacers. Fittings inside the elbows reduce the six-inch PVC to two-inch PVC. The advantage of this iteration is the symmetry and the center of mass along the center of the bike. The width between the handles was greater than 45 inches; therefore, the handlebars would not be in a comfortable position for the user to operate. This prompted the next design iteration that focused on decreasing the distance between the handles.

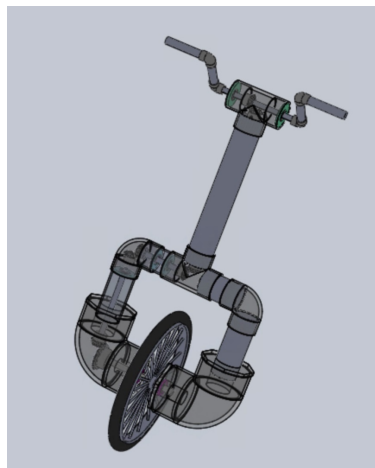


Figure 23: Third CAD Design - Asymmetrical Six-Inch Elbows

The above design features the same attachment to the wheel as the previous iteration. To decrease handle distance, several sets of miter gears are used to change direction of the torque applied to the shaft. In total, there are eight gears; three sets of miter gears, and one set of bevel gears that provide the gear reduction. In terms of design for manufacturability this design was

not reasonable. Ensuring four sets of gears mesh properly inside non-transparent PVC was going to be a difficult task. Therefore, the team had to redesign the assembly with the following constraints in mind that were learned through the iterative process:

- 1) The handles for cranking must be shoulder width apart.
- 2) The frame assembly must be relatively symmetrical.
- 3) The least number of gears possible must be used.

3.8 Final Design

3.8.1 Final Design of Hand Cycle

The above considerations led to the final design that was built to test as a prototype.

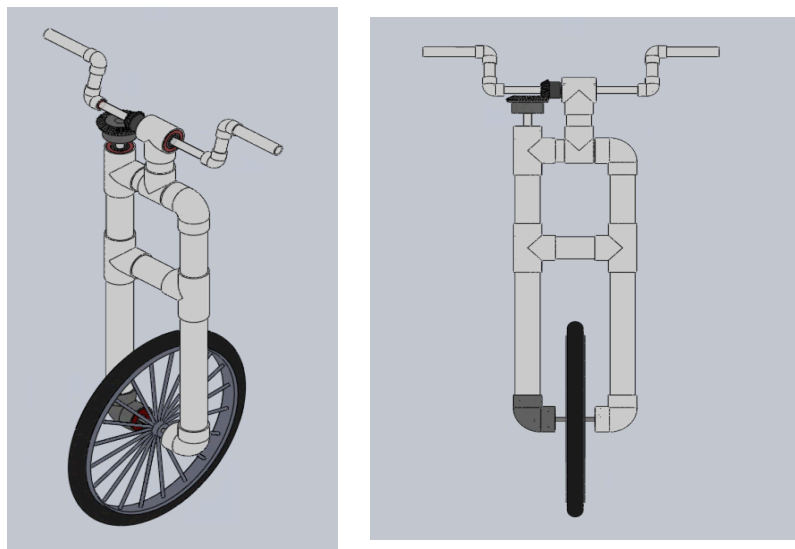


Figure 24: Isometric and Front View of Final Hand Cycle CAD Design

This design features four gears; one set of bevel gears at the top of the frame in a 2:1 assembly. The gears transmit the torque from the crankshaft to the drive shaft and one set of miter gears at the base of the frame transmits the torque from the drive shaft; this turns the wheel. Two-inch PVC pipe and fittings are used for the frame assembly and $\frac{3}{4}$ -inch PVC and fittings are used for the crank subassembly. The exposed gear design allows smaller PVC to be used because the large bevel gear does not have to be covered. During construction, the spacers had to be redesigned to increase their width to be thicker than the bearings. This provided more surface area so that the bearing could move within the spacer on the shaft to ensure the gears meshed properly.

3.8.2 Final Design of Attachment to Wheelchair

After the hand cycle design was completed, it was necessary to design the attachment mechanism to the wheelchair. For compatibility reasons, PVC pipe was chosen to make the attachability mechanism. The wheelchair donated to the group for the project was a classic hand

rim propelled chair. There were side flaps on the wheelchair, but these were removed so that attachment points could be mounted to the wheelchair.

The steering mechanism for the system was incorporated into the attachment. A hitch piece was designed such that a shoulder bolt through the two centerpieces would be the point of rotation. The hitch was designed such that it could be press fit into two-inch PVC fittings; however, this was deemed too large for the attachment frame work so reducer pieces were added to the hitch as shown below. The notch pieces had to be strengthened with epoxy due to the weak material properties of ABS 3D printed plastic that did not support the hand cycle in preliminary designs.

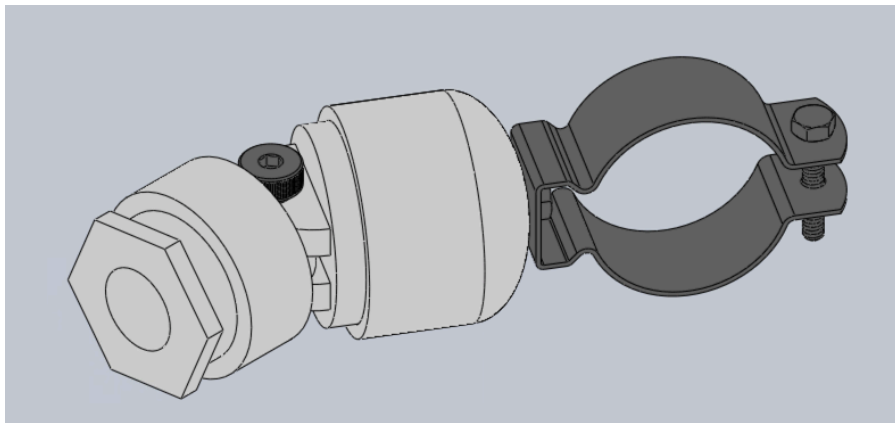


Figure 25: Steering Mechanism CAD Model

Using wye moveable angle clamps from McMaster-Carr, a $\frac{3}{4}$ -inch diameter PVC pipe frame as shown in the picture below was attached to the wheelchair and the hitch.

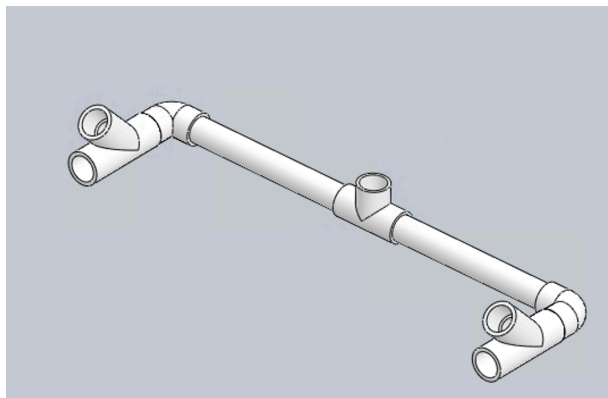


Figure 26: Attachment Framework CAD Model

3.9 Design Calculations

3.9.1 Gear Calculations

The basis of the design for the gear ratios was that the wheelchair and bike system would be able to operate up a hill on a 2-degree incline. There were several assumptions made to simplify this calculation and they are listed below:

- From ADA standards, five pounds is required as an input force to open doors and flush toilets
- The weight used was the world average of an adult
- All force applied to the crank is transmitted to the gears – no losses
- System is represented as a single block for force calculations
- Static friction is the coefficient between rubber tire and asphalt

The weight of the entire system was calculated and is shown in the table below.

Weight of Person	160	lbf
Weight of Wheelchair	35	lbf
Weight of Bike	15	lbf
Total Weight	210	lbf

Table 2: Weights of Components in System

The next step was to calculate the force produced at the wheel onto the ground using the total weight, gear ratio, input force, moment arm of input force and radius of the wheel. These calculations are shown below.

$$\begin{aligned} \text{Input Force by User} &= 5 \text{ lbf} \\ \text{Moment Arm of Force (Vertical Component of Crank)} &= 4.22 \text{ in} \\ \text{Moment applied at one crank arm} &= 5\text{lbf} * 4.22\text{in} = 21.1 \text{ lbf – in} \end{aligned}$$

$$\begin{aligned} \text{Number of Crank Arms} &= 2 \\ \text{Total Torque Applied on Crank} &= 42.2 \text{ lbf – in} \\ \text{Number of Teeth of Gear on Crank (Drive Gear)} &= 20 \\ \text{Number of Teeth of Gear on Drive shaft (Driven Gear)} &= 40 \end{aligned}$$

$$\text{Gear Ratio} = \frac{\text{Driven}}{\text{Drive}} = \frac{40}{20} = 2 : 1$$

The torque transmitted to the shaft is equal to the torque applied to the crank and the pinion gear, multiplied by the gear ratio.

$$\text{Total Transmitted to the Top of Shaft} = 42.2 \text{ lbf – in} * 2 = 84.4 \text{ lbf – in}$$

The shaft simply transmits the torque from top to bottom; therefore, the torque at the bottom of the shaft is equal to the torque at the top of the shaft. This is also equivalent to the torque applied to the wheel because miter gears are at the bottom with a (1:1) ratio. These gears simply change the direction of the torque.

$$\begin{aligned} \text{Total Transmitted to Bottom of Shaft} &= \text{Torque Transmitted to Top of Shaft} \\ &= \text{Torque Transmitted to Wheel} = 84.4 \text{ lbf} \cdot \text{in} \end{aligned}$$

The force applied at the ground is determined through the relationship of torque equals force multiplied by distance ($T = F * r$). In this case the distance is the radius of the wheel.

$$\text{Radius of Wheel} = 10 \text{ in}$$

$$\text{Force Applied at Ground} = \frac{T}{r} = \frac{84.4 \text{ lbf} \cdot \text{in}}{10 \text{ in}} = \mathbf{8.44 \text{ lbf}}$$

The next step was to complete a force balance on a 2-degree incline to determine the force required to move the wheelchair at a constant velocity. This was then compared to the force applied at the wheel, which had to be greater than the force to move the assembly at a constant velocity.

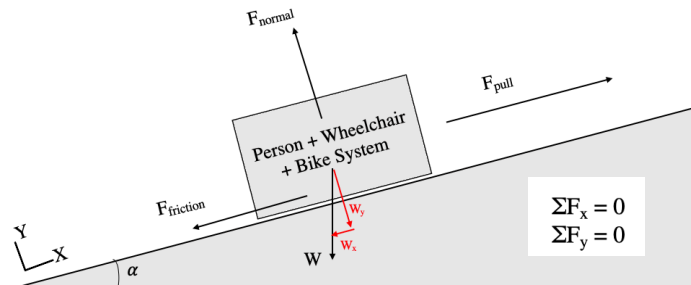


Figure 27: Free Body Diagram of System

$$\begin{aligned} W &= 210 \text{ lbs} \\ \alpha &= 2 \text{ degrees} = 0.034907 \text{ radians} \\ \mu_s &= 0.75 \end{aligned}$$

$$\begin{aligned} F_y : F_{\text{normal}} - W_y &= 0 \\ F_y : F_{\text{normal}} - W \cos \alpha &= 0 \\ F_{\text{normal}} &= W \cos \alpha \\ F_{\text{normal}} &= 210 \text{ lbs} * \cos(0.034907) = 209.87 \text{ lbf} \end{aligned}$$

$$\begin{aligned} F_x : F_{\text{pull}} - F_{\text{friction}} - W_x &= 0 \\ F_x : F_{\text{pull}} - \mu F_{\text{normal}} - W \sin \alpha &= 0 \\ F_{\text{pull}} &= \mu F_{\text{normal}} + W \sin \alpha \end{aligned}$$

$$\begin{aligned} F_{\text{pull}} &= (0.75 * 209.87 \text{ lbf}) + (210 \text{ lbf} \sin(0.034907)) \\ F_{\text{pull}} &= \mathbf{164.73 \text{ lbf} = 732.75 \text{ N}} \end{aligned}$$

Based on the above calculations it was determined that $F_{\text{pull}} > \text{Force Applied at Ground}$. This meant the current design of our bike could not overcome static friction up a 2-degree incline. This will be addressed in the commercialization and redesign chapter.

3.9.2 Stress Analysis (FEA)

After the design of the hand cycle was completed, stress analysis and Finite Element Analysis (FEA) were performed on the load and torque bearing parts of the assembly. Using the part models that were created for the CAD model, SolidWorks static simulation analysis feature was used to carry out this testing.

In many cases, the factor of safety was extremely high, meaning that in redesign and commercialization, smaller parts will be used. This will be helpful to reduce weight and size of the current prototype. The parts and subassemblies that were analyzed were: crank-shaft, drive shaft, miter gear tooth, bevel gear tooth, pinion gear tooth and frame subassembly.

Crank Shaft

The crankshaft is a $\frac{3}{4}$ -inch diameter nylon rod. The figure below shows the mesh on the model which was selected as the 50% mesh between coarse and fine for a total of 5100 elements.

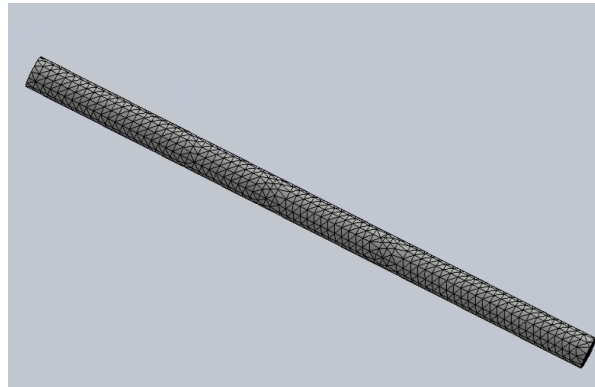


Figure 28: FEA Mesh Crankshaft

To properly analyze this part, it had to be split to apply the necessary loads in the appropriate places; the dimensions for the splits are shown below. The different sections are numbered such that in the loads table below, the number section aligns with the loads that were applied in that section.

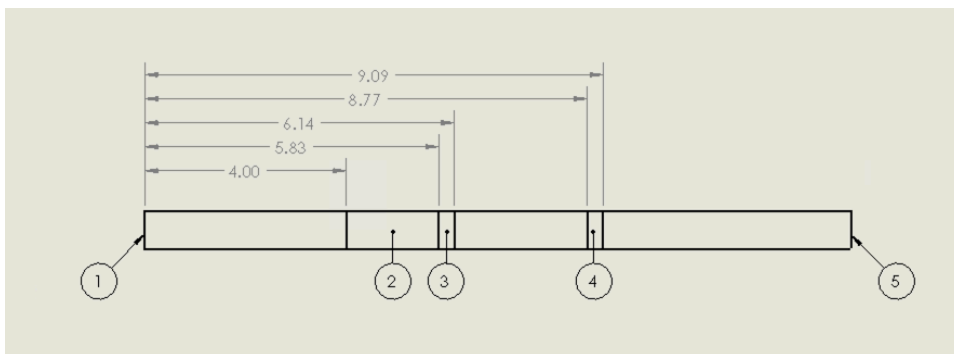


Figure 29: Split Dimensions of Crankshaft

For the purposes of this analysis, the table below shows the forces and moments that were applied. These are based off the calculations in the previous section. Several assumptions were made to complete this analysis:

- The location of the pinion gear was set as a fixed support.
- The loads on the end of the shaft that represent the “pedal” force are strictly moments; no additional downward force is applied on the shaft from the crank handles.

Location of Load	Type of Load	Magnitude	Direction
1	Moment	21 lbf in	Clockwise
2	Fixed	N/A	Clockwise
3	Bearing	N/A	--
4	Bearing	N/A	--
5	Moment	21 lbf in	--

Table 3: FEA Loads Crankshaft

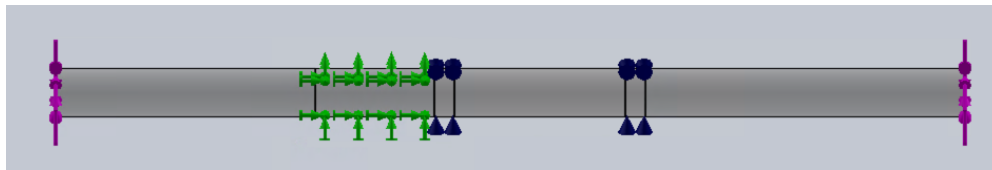


Figure 30: Loads Applied for Crankshaft FEA

The figure below shows the Von-Mises stress analysis results. Based on the yield strength, the factor of safety is roughly 29; therefore, the size of this shaft can be greatly reduced without compromising its integrity. According to this analysis, with the small force applied, the shaft should never fail. The table below summarizes the results of the analysis for the factors analyzed.

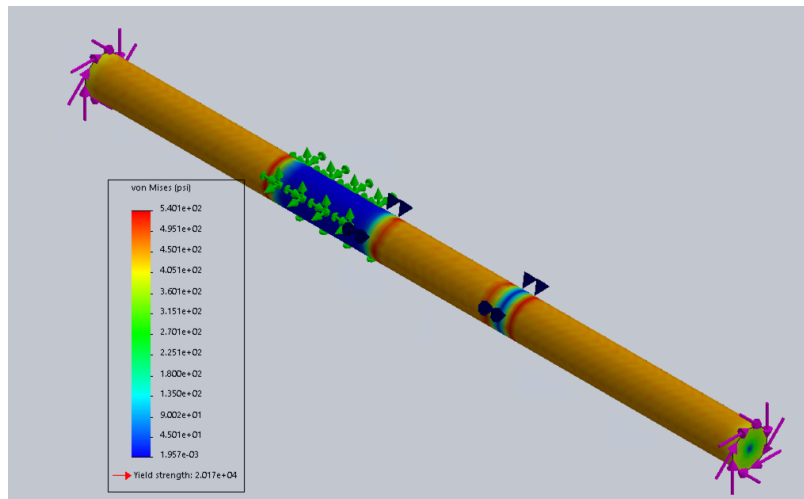


Figure 31: Crank Shaft Stress Analysis Results

	Minimum	Maximum
Von Mises Stress	0.001957 psi	540.1 psi
Displacement	0 in	0.004188 in
Strain	1.398×10^{-9}	3.381×10^{-4}

Table 4: FEA Results Crank Shaft

Drive Shaft

On top of the drive shaft is a large bevel gear and on the bottom is a smaller miter gear. The drive shaft is a $\frac{3}{4}$ -inch diameter nylon rod. The figure below shows the mesh on the model which was selected as 50% between coarse and fine for a total of 6729 elements.

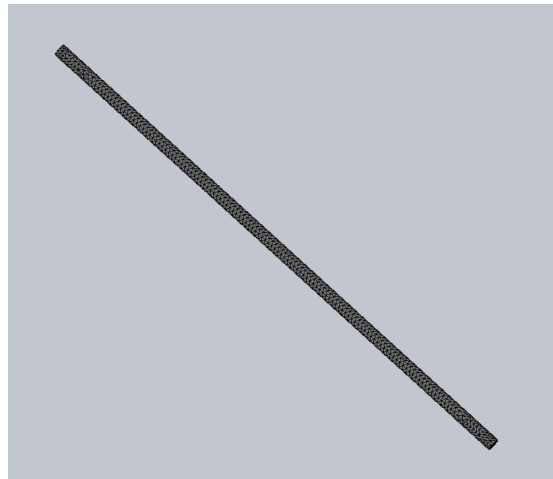


Figure 32: FEA Mesh Drive Shaft

To properly analyze this part, it had to be split to apply the necessary loads in the appropriate places; the dimensions for the splits are shown below. The different sections are numbered such that in the loads table below, the number section aligns with the loads that were applied in that section.

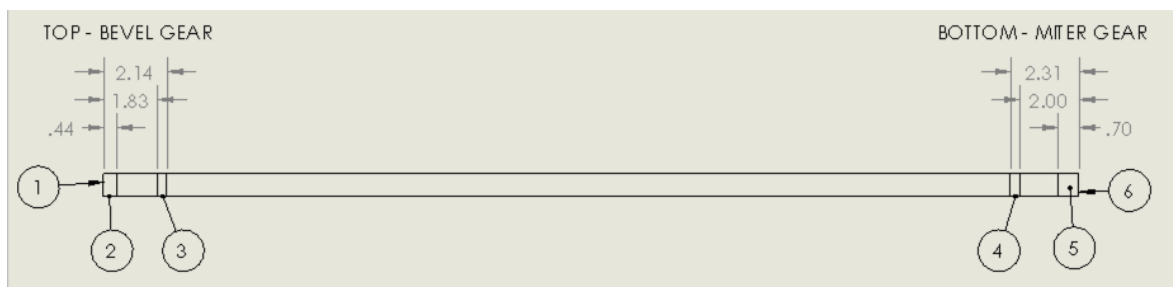


Figure 33: Split Dimensions of Drive Shaft

For the purposes of this analysis, the table below shows the forces and moments that were applied. These are based off the calculations in the previous section. Several assumptions were made to complete this analysis:

- The location of the bevel gear was set as a fixed support.
- The location of the miter gear was set as a fixed support.

Location of Load	Type of Load	Magnitude	Direction
1	Moment	84 lbf in	Clockwise
2	Fixed	N/A	--
3	Bearing	N/A	--
4	Bearing	N/A	--
5	Fixed	N/A	--
6	Moment	84 lbf in	Counterclockwise

Table 5: FEA Loads Drive Shaft



Figure 34: Loads Applied for Drive Shaft FEA

The figure below shows the Von-Mises stress analysis results. Based on the yield strength, the factor of safety is roughly 11; therefore, the size of this shaft can be greatly reduced without compromising its integrity. According to this analysis, with the small force applied, the shaft should never fail. The table below summarizes the results of the analysis for the factors analyzed.

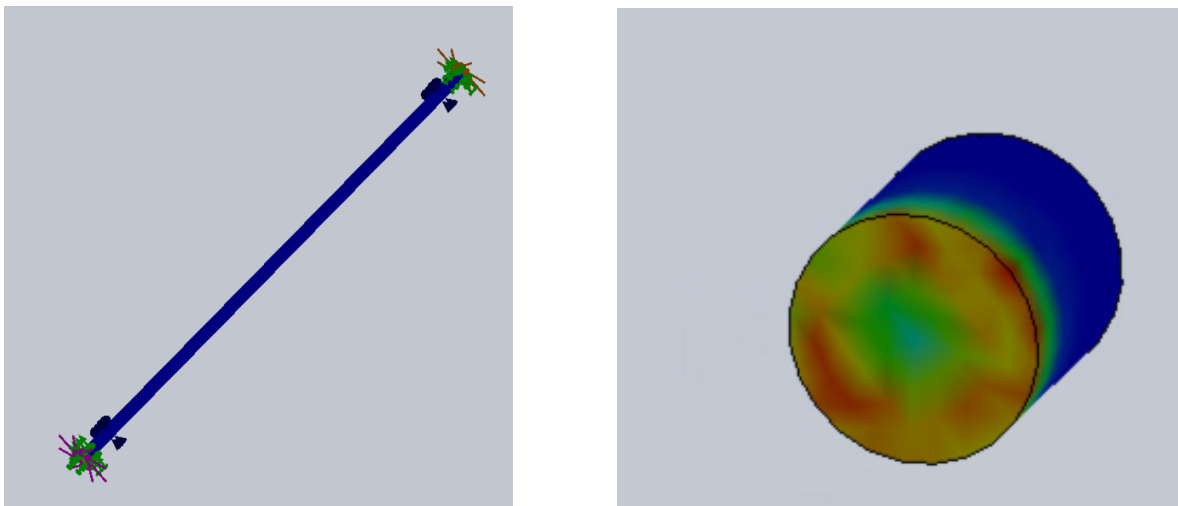


Figure 35: (L) Drive Shaft Stress Analysis Results; (R) Bottom View Shaft Stress Results

	Minimum	Maximum
Von Mises Stress	3.833×10^{-4} psi	1803 psi
Displacement	0 in	1.884×10^{-4} in
Strain	5.136×10^{-10}	1.019×10^{-3}

Table 6: FEA Results Drive Shaft

Bevel Gear Tooth

The bevel gear is mounted to the top of the drive shaft. The bevel gear is a 3D printed part of approximately 10% infill. This gear is meshed with a pinion gear on the crankshaft in a 2:1 ratio that transmits the torque to the bottom of the shaft. The figure below shows the mesh on the model, which was selected as 50% between coarse and fine for a total of 9640 elements.

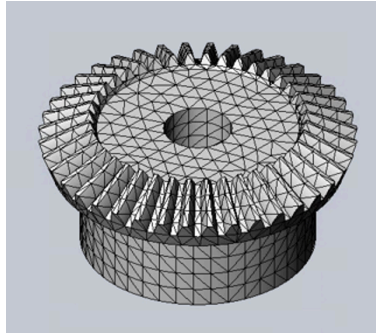


Figure 36: FEA Mesh Bevel Gear

To properly analyze this part, one gear tooth was selected. A force was applied to the side of the tooth equivalent to the torque on the gear, divided by the radius. The two places where loads were applied are numbered in the table below to correspond with the loads applied to that section.

$$\text{Torque Applied to Gear} = 84.4 \text{ lbf} \cdot \text{in}$$

$$\text{Radius of Gear} = \frac{\text{OD}}{2} = \frac{4.06 \text{ in}}{2} = 2.03 \text{ in}$$

$$\text{Force on Gear Tooth} = \frac{84.4 \text{ lbf} \cdot \text{in}}{2.03 \text{ in}} = 41.58 \text{ lbf}$$

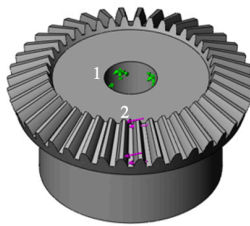


Figure 37: Loads Location Drawing Bevel Gear

For the purposes of this analysis, the table below shows the forces and fixtures that were applied.

Location of Load	Type of Load	Magnitude	Direction
1	Fixed	N/A	--
2	Force	41.58 lbf	Into Side of Tooth

Table 7: FEA Loads Bevel Gear

The figure below shows the Von-Mises stress analysis results. The yield strength of 3D printed ABS plastic is roughly 4,700psi. Therefore, the factor of safety on this gear tooth is roughly 6.5. However, it should be noted that this is just an estimate since the printed part is not full density, so the computer modeling is not entirely accurate. The table below summarizes the results of the analysis for the factors analyzed.

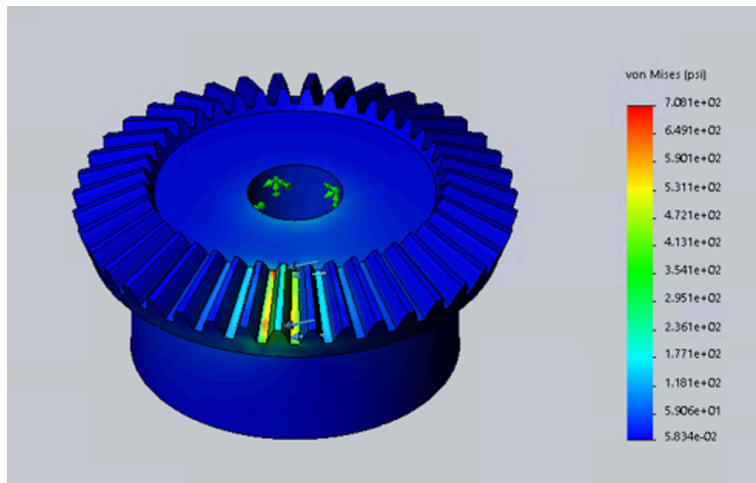


Figure 38: Bevel Gear Stress Analysis Results

	Minimum	Maximum
Von Mises Stress	0.05834 psi	708 psi
Displacement	0 in	2.008×10^{-3} in
Strain	3.185×10^{-7}	1.592×10^{-3}

Table 8: FEA Results Bevel Gear

Pinion Gear Tooth

The pinion gear is mounted to the crankshaft. It is a 3D printed part of approximately 20% infill. The gear is meshed with the bevel gear shown in the analysis above. The figure below shows the mesh on the model, which was selected as 50% between coarse and fine for a total of 7967 elements.

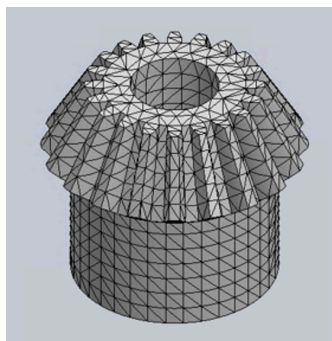


Figure 39: FEA Mesh Pinion Gear

To properly analyze this part, one gear tooth was selected. A force was applied to the side of the tooth equivalent to the torque on the gear divided by the radius as shown below. The two places where loads were applied are numbered in the table below to correspond to the number of loads applied to that section.

Torque Applied to Gear = 84.4 lbf – in

$$\text{Radius of Gear} = \frac{\text{OD}}{2} = \frac{2.24 \text{ in}}{2} = 1.12 \text{ in}$$

$$\text{Force on Gear Tooth} = \frac{42.2 \text{ lbf – in}}{1.12 \text{ in}} = 37.67 \text{ lbf}$$

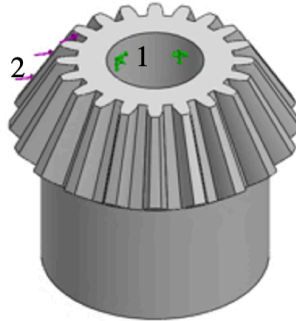


Figure 40: Loads Location Drawing Pinion Gear

For the purposes of this analysis, the table below shows the forces and fixtures that were applied.

Location of Load	Type of Load	Magnitude	Direction
1	Fixed	N/A	--
2	Force	37.67 lbf	Into Side of Tooth

Table 9: FEA Loads Bevel Gear

The figure below shows the Von-Mises stress analysis results. The yield strength of 3D printed ABS plastic is roughly 4,700psi. Therefore, the factor of safety on this gear tooth is roughly 6.8. However, it should be noted that this is just an estimate since the printed part is not full density, so the computer modeling is not entirely accurate. The table below summarizes the results of the analysis for the factors analyzed.

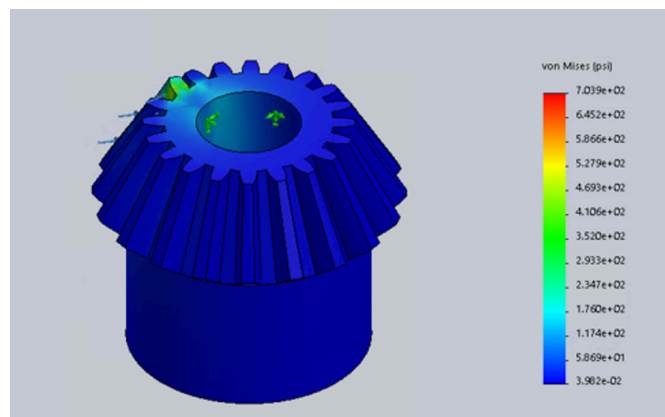


Figure 41: Pinion Gear Stress Analysis Results

	Minimum	Maximum
Von Mises Stress	0.03982 psi	703.9 psi
Displacement	0 in	1.344 x 10 ⁻³ in
Strain	7.920 x 10 ⁻⁸	1.667 x 10 ⁻³

Table 10: FEA Results Pinion Gear

Miter Gear Tooth

There are two miter gears in the assembly, used to change the direction of the torque from the drive shaft to the wheel axle. They are 3D printed parts of approximately 20% infill. The figure below shows the mesh on the model, which was selected as 50% between coarse and fine for a total of 8827 elements.

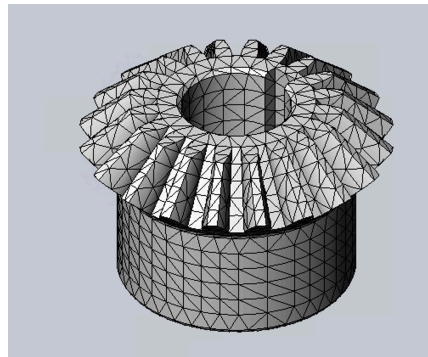


Figure 42: FEA Mesh Miter Gear

To properly analyze this part, one gear tooth was selected. A force was applied to the side of the tooth equivalent to the torque on the gear divided by the radius as shown below. The two places where loads were applied are numbered such that in the loads table below, the number section aligns with the loads applied to that section.

$$\text{Torque Applied to Gear} = 84.4 \text{ lbf} \cdot \text{in}$$

$$\text{Radius of Gear} = \frac{\text{OD}}{2} = \frac{1.06 \text{ in}}{2} = 1.12 \text{ in}$$

$$\text{Force on Gear Tooth} = \frac{42.2 \text{ lbf} \cdot \text{in}}{1.06 \text{ in}} = 39.8 \text{ lbf}$$

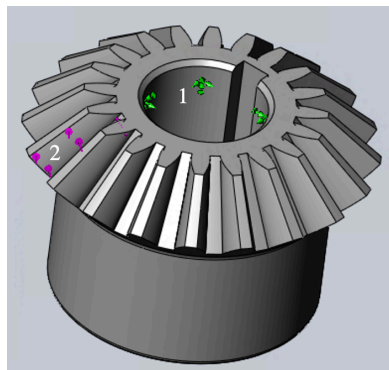


Figure 43: Loads Location Drawing Miter Gear

For the purposes of this analysis, the table below shows the forces and fixtures that were applied.

Location of Load	Type of Load	Magnitude	Direction
1	Fixed	N/A	--
2	Force	39.8 lbf	Into Side of Tooth

Table 11: FEA Loads Miter Gear

The figure below shows the Von-Mises stress analysis results. The yield strength of 3D printed ABS plastic is roughly 4,700psi. Therefore, the factor of safety on this gear tooth is roughly 4.4. However, it shall be noted that this is just an estimate since the printed part is not full density, so the computer modeling is not entirely accurate. The table below summarizes the results of the analysis for the factors analyzed.

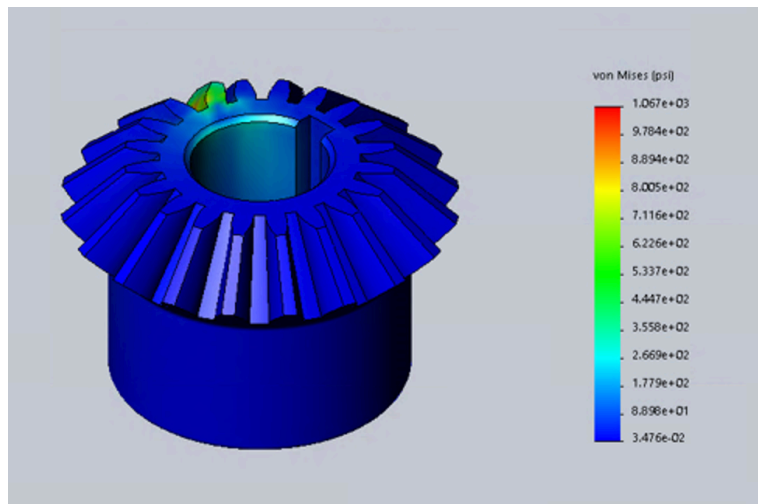


Figure 44: Miter Gear Stress Analysis Results

	Minimum	Maximum
Von Mises Stress	0.03476 psi	1,076 psi
Displacement	0 in	2.623×10^{-3} in
Strain	8.735×10^{-7}	3.332×10^{-3}

Table 12: FEA Results Miter Gear

Chapter 4: Prototype

4.1 Final Bill of Materials

Item	McMaster-Carr Part Number/ Description	Unit Price	Quantity	Total Price
2" PVC Elbow Connector - White	4880K26 – Standard – Wall PVC Fitting for Water, 90 Degree Elbow Connector, White, 2 Socket – Connect Female	\$1.82	2	\$3.64
2" PVC Elbow Connector - Clear	9161K26 – Unthreaded PVC Pipe Fitting for Water, Standard – Wall, 90 Degree Elbow Connector, Clear, 2 Socket Female	\$46.38	1	\$46.38
2" PVC T Connector – White	4880K46 – Standard – Wall PVC Pipe Fitting for Water, Tee Connector, White, 2 Size Socket – Connect Female	\$2.25	4	\$9.00
2" PVC T Connector – Clear	9161K36 – Unthreaded PVC Pipe Fitting for Water, Standard – Wall, Tee Connector, Clear, 2 Socket – Connect Female	\$57.16	1	\$57.16
2" PVC Pipe	48925K96 – Standard – Wall Unthreaded PVC Pipe for Water, 2 Pipe Size, 5 Feet Long	\$10.80	1	\$10.80
¾" PVC Pipe	48925K92 - Standard – Wall Unthreaded PVC Pipe for Water, ¾ Pipe Size, 5 Feet Long	\$3.30	1	\$3.30
¾" PVC Elbow Connector	4880K22 – Standard – Wall PVC Pipe Fitting for Water, 90 Degree Elbow Connector, White, ¾ Socket – Connect Female	\$0.35	6	\$2.10
¾" PVC T Connector	4880K42 – Standard – Wall PVC Fitting for Water, Tee Connector, White, ¾ Size Socket – Connect Female	\$0.44	1	\$0.44
¾" PVC Wye Connector	4880K637 – Standard – Wall PVC Pipe Fitting for Water Wye Connector, ¾ Pipe Size Socket – Connect Female	\$2.75	2	\$5.50
Bevel Gear	2515N19 – Bevel Gear, 0.710" Face Width – 3D Printed	\$2.50	1	\$2.50
Pinion Gear	2515N21 – Metal Bevel Pinion, 0.710" Face Width – 3D Printed	\$1.50	1	\$1.50
Miter Gear	6843K19 – Miter Gear, Keyed Bore, 10 Pitch, 20 Teeth, for ¾" Shaft Diameter – 3D Printed	\$0.51	2	\$1.02
Nylon Rod (Shaft and Crank)	8538K21 – Off – White Nylon Rod, ¾" Diameter, 5 Feet Long	\$2.46	1	\$2.46
Bearings (Shaft and Crank)	60355K507 – Ball Bearing, Open, Trade Number R12, for ¾" Shaft Diameter	\$7.92	4	\$31.68
Shoulder Bolt	91259A714 – Alloy Steel Shoulder Screw, ½" Shoulder Diameter, 1-1/4" Shoulder Length, 3/8 -16 Thread	\$2.57	1	\$2.57
Axle	1482K11 – Rotary Shaft 1566 Carbon Steel, 10mm Diameter, 200 mm Long	\$7.80	1	\$7.80
Bearings (Axle)	5972K94 – Ball Bearing, Open, Trade Number 6000, for 10mm Shaft Diameter	\$6.78	2	\$13.56
Spacer for Fitting	3D Printed	\$0.38	3	\$1.14

(Crank and Shaft)				
Spacer for 2" Pipe	3D Printed	\$0.35	1	\$0.35
Spacer for Fitting (Axle)	3D Printed	\$0.64	2	\$1.28
Metal Clip	Threaded – Rod – Mount Clamping Hanger with Closure Bolt and Nut, 304 Stainless Steel, 2 – 3/8" ID	\$5.51	1	\$5.51
Bike Tire	20" Diameter Bicycle Tire	Donated	1	Donated
Wheelchair	--	Donated	1	Donated
Hitch	3D Printed	\$1.25	1	\$1.25
Metal Wheelchair Attachment Points	2534T33 - Clamp-on Framing Fitting, Adjustable – Angle Wye Through – Hole Connector for 1" Rail OD	\$6.40	4	\$25.60
			Total Price	\$235.90

Preparing the Wheel

A ten-millimeter carbon steel rod was secured inside the inner diameter wheel hub with steel putty and steel epoxy. Once this rod was secured on both sides, a ball bearing, and spacer were secured to the axle on either side of the wheel. A 3D printed spacer and plastic epoxy were used to fix the gear to the axle so that the gear and wheel moved simultaneously. A two-inch clear elbow was placed over the gear to provide easy attachment to the drive shaft mechanism. The clear elbow was used for enhanced visibility of the gears meshing. An opaque elbow was used on the non-gear side.



Figure 45: Preparing the Wheel

4.2 Bike Construction

Assembling Drive Shaft

The nylon drive shaft had two ABS 3D printed gears press fit to each end. The miter gear at the bottom of the shaft has a two-inch pitch diameter and 20 teeth. The bevel gear at the top of the shaft has a four-inch pitch diameter and 40 total teeth. For assembly purposes, only the bottom gear was attached at this time.

Constructing the Frame

A symmetrical frame was created from two-inch diameter PVC. A 14-inch long PVC piece was attached to the elbow not containing the gear. On the opposing side, another 14-inch PVC piece was used. A ball bearing and 3D printed spacer were inserted into the bottom of the PVC pipe. The shaft was then inserted into the ball bearing until the gear was almost flush with the bearing. This piece was then placed into the clear elbow until the gears meshed. Attached to the other end of the 14-inch pieces were two PVC Tee connectors and a horizontal piece of PVC connecting the two sides. From the point of connection, coming off the Tee connectors and continuing vertically were two pieces of eight-inch long PVC. On the side that does not contain the shaft, a PVC elbow connector attaches directly to the crank assembly. On the side with the shaft, a clear PVC Tee connector contained a ball bearing and 3D printed spacer on the top socket. The large bevel gear was placed on the end of the shaft coming out of the clear Tee using appropriate adhesives. Between the two sides is a Tee connector with the middle socket facing up.

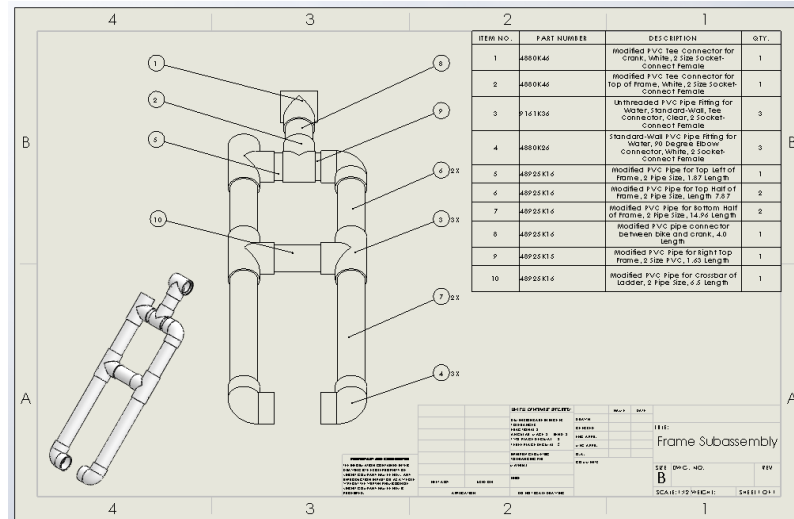


Figure 46: Frame Subassembly Drawing and BOM

Assembling Crank

Once the shaft was constructed, the crank was then configured based off the height of the shaft and the distance the gears needed to mesh. Ball bearings and spacers were placed into the two ends of a PVC Tee connector. A 14-inch nylon rod was placed through the ball bearings and approximately centered. The pinion bevel gear was press fit onto the rod to mesh with the bevel gear on top of the drive shaft. Two small 3D printed spacers and $\frac{3}{4}$ -inch PVC elbows were placed on the ends of the rod. Using $\frac{3}{4}$ -inch pipe and elbows, the hand pedals were constructed in the configuration below.

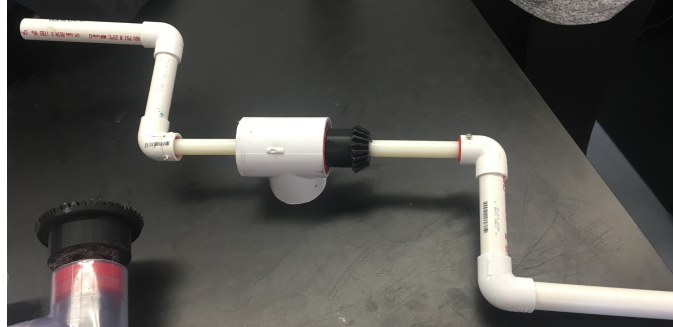


Figure 47: Crank Configuration

A small length two-inch PVC pipe was used to connect the inverted Tee on the bike to the crank mechanism shown below.

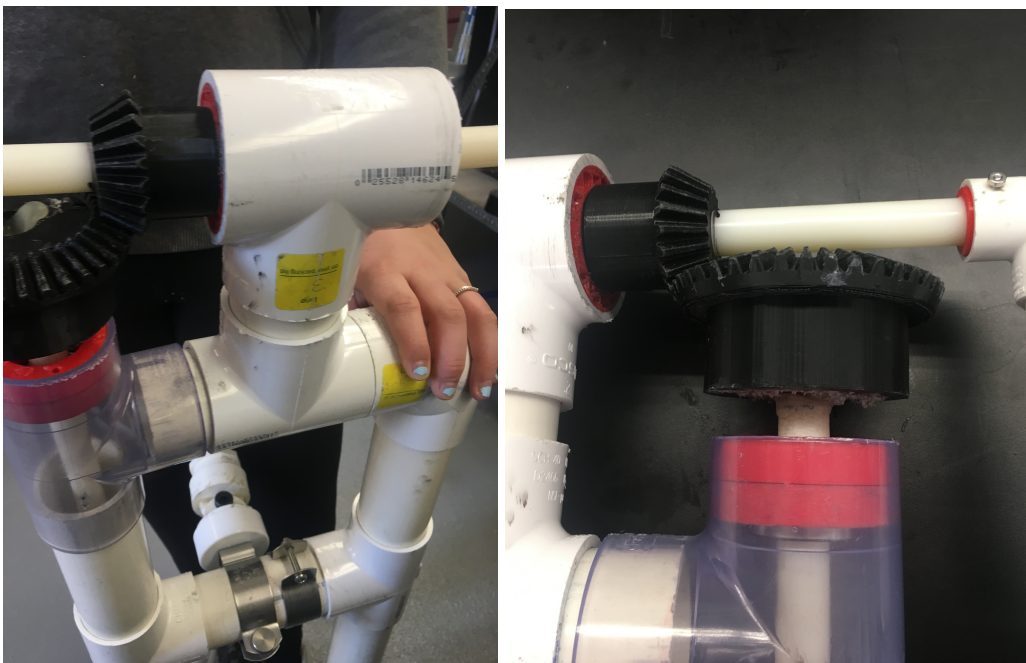


Figure 48: Crank Connection to Bike

4.3 Attachment Mechanism Construction

On the cross bar of the bike frame, a hitch mechanism was attached that connected the bike to the wheel chair. This hitch mechanism consisted of a metal ring that was attached to the PVC cross bar. Using a bolt and PVC cap, the metal ring was connected to half of the hitch. A PVC reducer was fit into the other half of the hitch. These two halves were connected using a shoulder bolt which serves as the pivot point for steering.



Figure 49: Steering Hitch

Attached to the wheelchair are four steel adjustable-angle wye clamps, shown in the figure below. Two clamps were attached with steel putty on either side of the wheelchair. The angle of these clamps can be adjusted using Allen wrenches.



Figure 50: Wye Connector Secured to Wheelchair

Connected to the wye clamps are two-inch lengths of $\frac{3}{4}$ -inch PVC which were secured using nuts and bolts. These sections of pipe were joined together in a wye union, that feeds into 3.5-inch long PVC with elbows at their other ends. Two pieces of 8.5-inch long PVC connected these elbows to a Tee at the center of the wheelchair. The steering hitch, described in the section above, connects this PVC structure to the bike. The photo below shows this PVC configuration.



Figure 51: Configuration of PVC Connection



Figure 52: Complete Prototype Assembly

Chapter 5: Prototype Field Testing

Once the team finished constructing the prototype, they tested the bike to determine how it performed. The goal of the prototype was to be a functional arm bike that could propel an individual with minimal effort that could navigate a typical outdoor environment. The team evaluated if the user could start the arm bike without assistance, brake within a reasonable distance and steer to avoid obstacle. In addition, they measured distance traveled to determine the speed of the bike. While small samples of testing were conducted throughout the construction of the device, one official day was spent testing the finalized prototype. This testing was completed exclusively by team members and was conducted per the protocol described in this section.

All testing was done outside on the WPI Quad and by the Bartlett Center. One team member sat in the wheelchair and propelled themselves using only the arm bike attachment. They operated the device and moved exclusively using their upper body to simulate the capabilities of the target user. A different member of the team served as an assistant, ensuring the wheelchair user was safe and providing support with starting, stopping, and maneuvering as necessary. During testing one team member took photographs, one member recorded qualitative observations, and one member collected numerical data including time and distance values.

Six trials were completed: three on a two-degree decline and three on relatively flat ground. Each individual trial consisted of the following steps. First the user attempted to propel themselves starting from rest. If they were able to overcome static friction without assistance, this was recorded, and if not, the assistant applied a force to propel forward. Once they began moving, a different team member timed how long it took to travel some distance over ten and fifteen meters. The distance and time were recorded and used to calculate velocity values. Next the individual tested the steering capabilities, turning the bike as far left and right as possible until a 90-degree turn was completed. The turning radius was measured as the horizontal displacement, as shown in the diagram below.

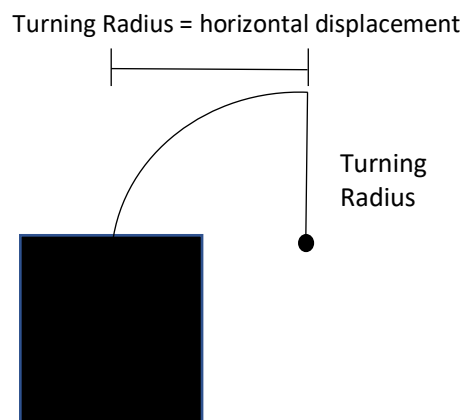


Figure 53: Turning Radius Diagram

Finally, the braking capabilities of the device were tested. The user would receive a force from the assistant, and after one second of moving, the user would grasp the crank and prevent rotation, to prevent the front wheel of the device from turning. If the bike came to a stop, brakes passed, if not, brakes failed. This step concluded one trial. Photos from this testing data can be found below.



Figure 54: Photos from Testing the Prototype

Data from these six trials are shown in the tables below. No trial performed well in all categories measured; however, there were varying levels of success for each aspect of the testing. The results suggested that the bike was capable of movement ranging from about 0.5-1.0 m/s, depending on the slope of the terrain being navigated. The brakes failed in all but two trials, as the gears experienced slippage. This prevented braking of the system through our device, meaning the classic brakes on the wheelchair were necessary. One positive aspect of the data were the turning radius values, of which the average was 1.45 meters. This was less than the team was anticipating, suggesting the wheelchair can make sharper turns in smaller areas.

Trial Number	Able to Start Without Assistance (Y/N)	Time (s)	Distance (m)	Speed (m/s)	Braking (Pass/Fail)	Turning Radius (m)
1	N	15	13.41	0.89	Fail	1.5
2	N	13	11.89	0.91	Fail	1.4
3	N	15.8	12.80	0.81	Pass	1.6

Table 13: Raw Data from Testing on Bartlett Ramp

Trial Number	Able to Start Without Assistance (Y/N)	Time (s)	Distance (m)	Speed (m/s)	Braking (Pass/Fail)	Turning Radius (m)
1	N	15	10.1	0.67	Pass	1.4
2	N	13	11.2	0.86	Fail	1.5
3	N	14.8	10.8	0.73	Fail	1.3

Table 14: Raw Data from Testing on Quad

While testing, the team observed that the bike had difficulty supporting its own weight, making the angle of the bike difficult to control. This made cranking the handles a challenge, since the user's elbows hit the wheelchair arms. Additionally, the team noted that the bike's

connection to the front wheel was rather loose, causing motion of the bike frame during propulsion. While this did not greatly impact the performance of the bike, it did make it slightly more difficult to control. Another challenge faced during testing was gear misalignments that prevented the drive shaft and wheel axle from meshing. This prevented transmission of motion from the crank to the wheel, invalidating the trial since the bike was only moving as a result of gravity or momentum. Finally, the team noted that there were several connections that would benefit from improved adhesion or attachment for future test trials.

One positive feature the team observed during testing was the hitch mechanism provided ease and improved extent of steering. Turning the bike required minimal effort and the bike's response was faster and more complete than the team anticipated. Additionally, the team was pleased with the overall appearance of the bike. While there were concerns that the bike would appear too cumbersome and unappealing for use, the team found it was comparable in appearance to bikes currently on the market.

Chapter 6: Design Validation

To evaluate the success of the project, the team's original project goal and design parameters were used as a guide. If the original specification set by the team was met by the final prototype, this aspect of the design was deemed successful. If the specification of the team was not met, this aspect of the bike was a failed parameter. Discussions of the outcomes for each parameter including positive features, drawbacks, and places for improvement are discussed below.

Design Parameter #1- *Bike can be attached to most standard manual propulsion wheelchairs:* PASS

The attachment of the bike to the wheelchair used a combination of PVC pipes, PVC connectors and four adjustable-angle wye steel clamps as discussed in section 4.3 above. The wye clamps were permanently attached to the chair first by tightening them as far as possible using an Allen wrench. Steel putty was then used on all four clamps to permanently secure them into place on the wheelchair. Due to the clamps' ability to be loosened and tightened using an Allen wrench, most common wheelchair frames are compatible with the attachment mechanism. Although our attachment mechanism did pass this design parameter, the team experienced some difficulties. Firstly, to secure the PVC pipe into the metal clamps, bolts and nuts were utilized, making it difficult and time consuming to undo the bike attachment. This could be challenging for users with decreased fine motor skills since they must screw and unscrew four small nuts and bolts every time, they attach the bike to their wheelchair. Another long-term issue regarding the prototype is the use of steel putty for permanent attachment of the clamps. This putty was very strong for the construction and testing of the prototype, but for long term use other options such as welding should be explored to ensure stability of the clamps.

Design Parameter #2- *Bike avoids the use of chains, which are known for the propensity for derailment:* PASS

To overcome some of the complications experienced by users of chain driven hand bikes, the team implemented a drive shaft propulsion system. The details regarding the drive shaft construction can be found above in Section 4.2. When fully assembled and not under load, the drive shaft system was successful in propelling the prototype. The 3D printed gears meshed properly and created smooth operation of the drive system. The team was successful in creating a prototype that eliminated the need for bike chain propulsion. Problems in the drive shaft system arose when loads were applied to the prototype. When the weight of the user and the wheelchair were added to the prototype, the gears slipped. Failure of the drive shaft system was also experienced when the user applied a large force to the crank, sometimes causing a bearing to slip out of the spacer.

Design Parameter #3- *Bike can last for a minimum of five years: FAIL*

Due to material and time restrictions, the prototype was not constructed to last a minimum of five years. PVC is not a strong or reliable material to use in long-term dynamic applications. The frame experienced unnecessary movement during testing, causing problems with maintaining the correct angle and overall position of the bike. The adhesives used by the team were also a temporary solution for the prototype. Although a mix of plastic and steel epoxies was successful in the construction and testing of the prototype, for long-term use more permanent adhesion would be necessary. If the prototype had been built with enhanced materials and adhesions, the bike would likely last five years.

Design Parameter #4- *Bike costs less to manufacture than \$750: PASS*

The construction of the prototype cost a total of \$235. The team was able to keep the cost of the prototype low by using lower quality material and manufacturing methods than would be used in the real product. In creating the prototype, all four gears were 3D printed, which significantly reduced the cost. Selecting PVC as the frame material also contributed to the low cost, as PVC can be obtained in bulk for low prices. Although the team was able to assemble a prototype for under \$750, a bike designed for long-term use would not be constructed for such a small price.

Design Parameter #5- *Bike can start from rest with less than or equal to five pounds of input crank force: FAIL*

When completing calculations, the team found that with the current design, the prototype would not be able to overcome static friction on its own. This was further proven through testing conducted on the prototype. Even when the user applied maximum possible force to the crank static friction was not overcome, a slight push was needed to begin motion. The prototype could overcome rolling friction and propel the user forward, once motion began. The use of enhanced materials and a higher gear ratio would allow future arm bike designs to exceed static friction on their own with less than five pounds of force.

Design Parameter #6- *Bike can travel at least at two m/s: FAIL*

The prototyped hand bike cannot reach speeds of at least two m/s. Due to the low force needed to operate the crank, to achieve high speeds, the bike would need to be pedaled extremely fast. The prototype also does not have the ability to change gear ratio, therefore users cannot manually change the pedaling speed. These limitations restricted our bike to operation between only 0.5-1.0 m/s.

Design Parameter #7-*Bike weighs less than 20 pounds*: PASS

The bike constructed weighs approximately 15 pounds total. That is within our designated design parameter and would allow for wheelchair users to handle the bike with ease.

Design Parameter #8- *Bike is steerable with a one to two-meter turn radius*: PASS

The designed hitch used for steering allowed the prototype to operate within the one to two-meter turn radius range. The hitch design and construction provided an observed 1.4-1.6-meter turn radius. Overall steering of the prototype was easily operated with a low force and was responsive to the user's movement. A one-meter turn radius is still rather large, however, so for future considerations a smaller turn radius would be ideal to allow for improved navigation and obstacle avoidance.

Design Parameter #9- *Bike can brake and safely stop within three seconds*: FAIL

The current prototype does not have a brake system integrated on the bike. Instead, the user must either use their wheelchair brakes or tightly grasp the crank and hold it in one position to stop the drive shaft and slow down the wheel. The use of wheelchair brakes is not ideal due to the distance the user's hands would have to travel to go from the handles to the brakes. In the case of an emergency stop, this would waste time and compromise the safety of the user. Attempting to stop the bike through applying a stopping force on the crank is also not an optimal form of braking. Depending on the speed of the bike, this could result in a very high force needed to stop the crank. This form of braking is not reliable or consistent and may cause skidding. To ensure the safety of the user, a redesigned version of the arm bike would incorporate a reliable hand braking system.

Design Parameter #10- *Bike is portable and collapsible*: FAIL

Restrictions in time and materials resulted in the prototype not being portable or collapsible as intended. As it stands now, the arm bike lacks a folding feature, making storage and transportation a challenge. Collapsibility and portability would be a further consideration for future arm bike designs.

Chapter 7: Recommendations and Redesign

The prototype the team constructed proved the theory behind the chainless design, however budget and time limitations prevented the arm bike from being a realistic product. Despite the failures and shortcomings of the prototype, if adapted to better materials and manufacturing processes, the current challenges could be mitigated, and the design could result in a marketable device. The following section outlines how the team would redesign and construct an enhanced version of the prototype.

7.1 Propulsion System

As described in the design calculations and testing sections, the prototype could not overcome static friction with five pounds of force added to the wheelchair. This was due to a low gear ratio, resulting in insufficient force transmitted to the ground and wheel interface. Therefore, it was necessary to increase the gear ratio for a redesigned model. Using the previously calculated 165 pound-force required to overcome static friction, (rounded to 168 for a conservative estimate) the new gear ratio is calculated below.

$$\begin{aligned}\text{Force at Ground} &= 168 \text{ lbs} \\ \text{Radius of Wheel} &= 2.5 \text{ in} \\ \text{Torque at Center of Wheel} &= F * r = 168 \text{ lbs} * 2.5 \text{ in} = 420 \text{ lbf} - \text{in}\end{aligned}$$

The implementation of a miter gear to change torque direction from the wheel axle to the drive shaft will remain at the bottom of the assembly. Therefore, torque applied at the wheel is equal to the torque transmitted to the bottom of the drive shaft, which is also equal to the torque transmitted to the bevel gear at the top of the shaft.

$$\begin{aligned}\text{Torque at Center of Wheel} &= \text{Torque at Bottom of Shaft} \\ &= \text{Torque of Bevel Gear at Top of Shaft} = 420 \text{ lbf} - \text{in}\end{aligned}$$

The length of the vertical crank arm remains unchanged in the redesign because this length was found to be comfortable for the user. Thus, the torque generated at the crank from the five pounds of input force remains unchanged at 42.2 lbf – in. Using the definition for gear ratio, the two torques can be related to find the necessary gear ratio as shown below.

$$\begin{aligned}\text{Torque at Bevel Gear (Driven)} &= 420 \text{ lbf} - \text{in} \\ \text{Torque of Crank (Drive)} &= 42.2 \text{ lbf} - \text{in} \\ \text{Gear Ratio} &= \frac{\text{Torque of Driven Gear}}{\text{Torque of Drive Gear}} = \frac{420 \text{ lbf-in}}{42.2 \text{ lbf-in}} = 9.95 = 10:1\end{aligned}$$

This is a relatively high gear ratio and would require a large gear which would not fit within the constraints. Therefore, other options had to be explored. A right-angle speed reducer was an option which works by reducing shaft speed and increasing torque while transmitting motion at a 90-degree angle. The image below is an example of one. However, the required

output torque and speed ratio meant the box had to have dimensions of 7.75-inches by 6.75-inches by 5.75-inches which is too large to fit into the assembly.

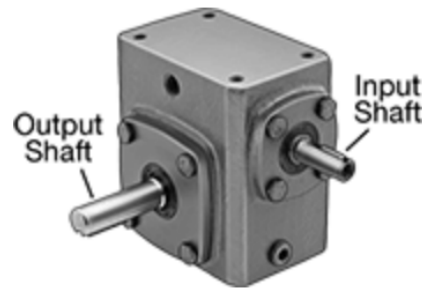


Figure 55: Right Angle Speed Reducer [28]

Another possible option is an inline speed reducer. This would slightly change the set-up of the frame of the bike but would allow the necessary speed reduction without a bulky gear box. There are different types of these available, but for cost purposes, a gearbox from Amazon was selected. The output shaft is keyed and there is an opening for the input shaft to be placed into. The overall dimensions for this reducer are 5.25-inches long by 3.5-inches wide by 3.5-inches tall.

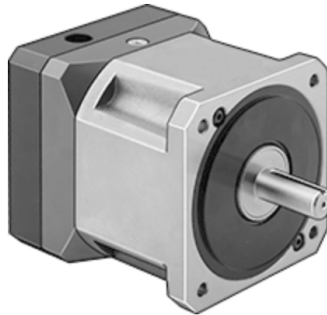


Figure 56: Inline Planetary Speed Reducer [28]

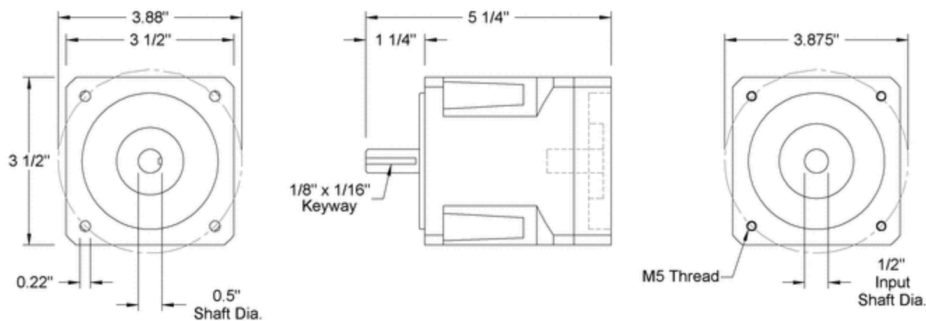


Figure 57: Engineering Drawing of Parallel Speed Reducer [28]

The new propulsion system subassembly would look similar to the figure below. A set of miter gears would change the torque direction from the crank to the shaft. The shaft would be split part way down, and a bracket would be welded to the gear box. The input shaft would then be welded into the gear box. A shaft coupling would be used to attach the output shaft of the gear

box to the remaining portion of drive shaft. A miter gear would be held to the bottom of the shaft with a key. Another miter gear would be attached to the keyed axle that would be welded to the wheel.

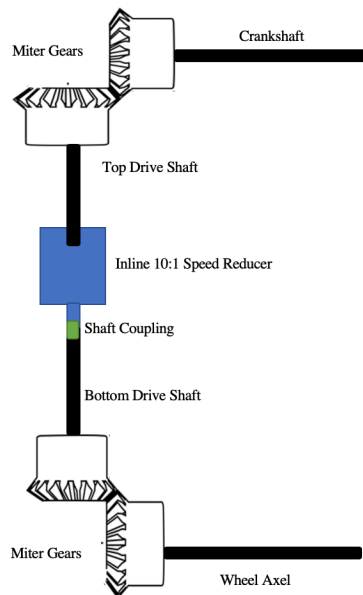


Figure 58: Redesign Propulsion System Schematic

An $3/8$ -inch aluminum shaft was chosen because it is lightweight but able to undergo the required torque without deformation or failure. Two 12-inch shafts would be purchased which would be cut to their appropriate length to fit in the assembly. For the output of the gear box, a shaft coupling is necessary to hold the shafts together. For the input, the gear box requires a 0.5-inch diameter shaft, so a step shaft is required. There is not one available with the necessary dimensions on McMaster-Carr, but a custom shaft could be machined. The price of the shaft in the table is estimated based off a slightly oversized step shaft from McMaster-Carr.

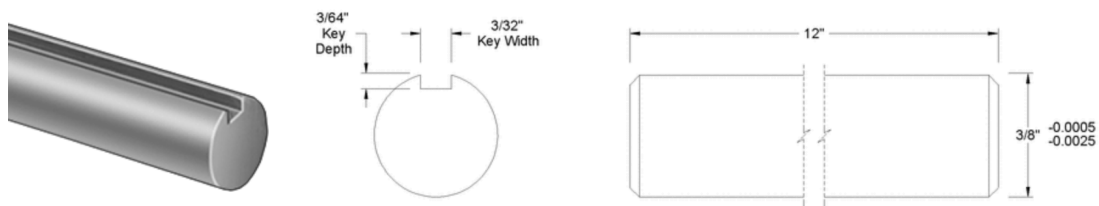


Figure 59: Output Redesign Shaft and Drawing [28]

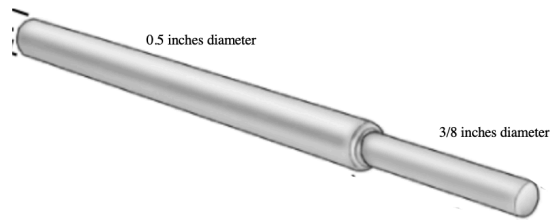


Figure 60: Input Redesign Step Shaft [28]

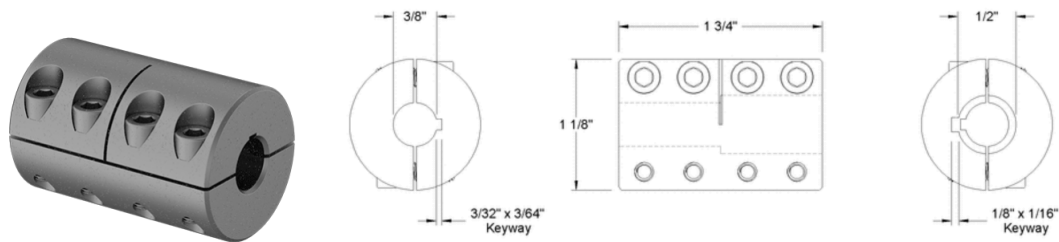


Figure 61: Shaft Coupling Figure and Drawing [28]

Four miter gears are required for this assembly. Based on parts available from McMaster-Carr, the smallest miter gear with a 3/8-inch shaft diameter is shown in the figure below. The outer diameter (OD) of this gear is 1.09-inch, therefore the aluminum tubing for the frame can have an inner diameter (ID) of 1.25-inch to enclose the bottom miter gears. The selected frame tubing will be discussed further below but has a 1.277-inch ID.

There will be four ball bearings for support, spread throughout the length of the shaft. The selected bearings have an 7/8-inch OD. The frame tubing has an ID of 1.277 inches. Therefore, spacers will be machined out of aluminum and welded into the frame where the bearings are to hold them into place.

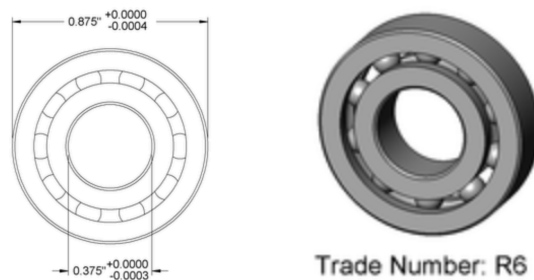


Figure 62: Shaft Ball Bearings Redesign [28]

There will be an axle that is press fit into the wheel hub. The hub of the wheel will not have bearings in it so that it is a direct drive with no free wheel capabilities. The selected wheel is made of polyurethane and can be used on asphalt, brick and concrete surfaces. It has an axle diameter of 3/8 inches therefore the same bearings as the drive shaft will be used.

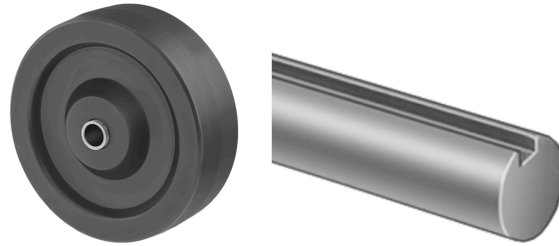


Figure 63: Wheel and Axel Redesign [28]

7.2 Hand Crank

The crank handles will be made from the same material as the frame and will have a rubber coating on the end of each handle for a better grip. The hand crank will have the same geometry as the existing prototype, but each handle will have a pin that will allow for the rotation to be changed between asynchronous and synchronous.

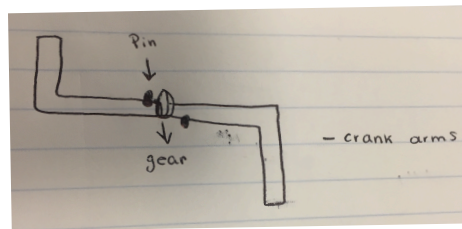


Figure 64: Hand Crank Sketch Redesign

7.3 Brakes

A single hand brake utilizing a cable running from a lever on the shaft will pull the two levers on the brakes together will be used. There will be two brake pads against the outside of the wheel that are squeezed by the levers. This brake will be mounted on the middle of the drive shaft frame.



Figure 65: Brakes Redesign [22]

7.4 Steering

The steering capability of the bike and wheelchair assembly will come from a two-piece hitch with one side welded to the bike and the other side welded to the attachability frame that extends from the wheelchair. The new design will have the hitch machined out of aluminum and be placed closer to the wheelchair to increase turn radius.

7.5 Frame

The frame will be 1.375-inch diameter aluminum tubing and be in the same geometry as the prototype. All pieces will be adhered together using Tungsten Inert Gas welding. To be compact, a telescoping rod and clamp will be used similar to that of the Rio Dragonfly arm bike. This would also give the user the ability to alter the height.



Figure 66: Rio Dragonfly Chain Drive with Telescoping Feature [22]

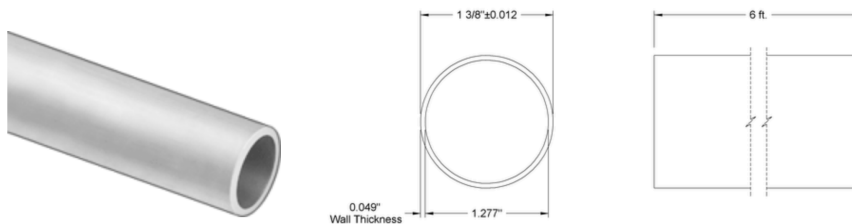


Figure 67: Frame Tubing Redesign [28]



Figure 68: Dragon Plate Telescoping Tube Clamp [20]

7.6 Attachability

The attachability mechanism for the redesign was modeled off of the Dragonfly Handcycle which is shown below. This mechanism features four ball clamps. These clamps tighten directly onto the front frame of the wheelchair. The configurations of the clamps and their connectors cause the front wheels to slightly lift off of the ground. Bottom and top link wings are used to secure this position.



Figure 69: Dragonfly Handcycle Attachment Mechanism [27]



Figure 70: Location of Ball Clamps on Wheelchair Frame [27]

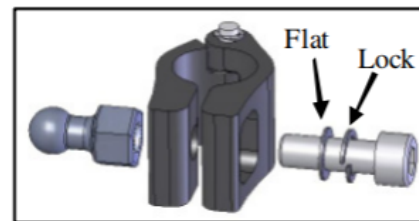


Figure 71: Ball Clamp Parts [27]

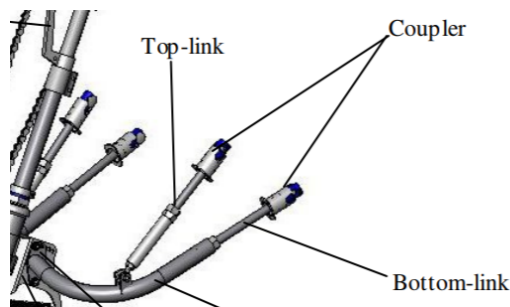


Figure 72: Location of Bottom and Top Links and Couplers [27]

7.7 Redesign Bill of Materials

Part	Purchase Location	Unit Price	Quantity	Total Price
Gear Box	Amazon – 10:1 Ratio Planetary Reducer Stepper Speed Reducer for NEMA 34 Stepper Motor P/N: 64815K53	\$61.00	1	\$61.00
Output Drive Shaft	McMaster-Carr - Lightweight Keyed Rotary Shaft 2024 Aluminum, 3/8" Diameter, 12" Long P/N: 1570K32	\$18.38	1	\$18.38
Input Drive Shaft	Custom Step-Down Rotary Shaft. 1/2" Diameter, One End with 3/8" Step, 12" Long	\$23.78	1	\$23.78
Miter Gears	McMaster-Carr - Metal Miter Gear Keyed Bore, 16 Pitch, 16 Teeth, for 3/8" Shaft Diameter P/N: 6843K11	\$50.66	4	\$202.64
Bearings for Shaft	McMaster-Carr - Ball Bearing, Open, Trade Number R6, for 3/8" Shaft Diameter P/N: 60355K504	\$5.78	4	\$34.68
Axle	McMaster-Carr - Lightweight Keyed Rotary Shaft 2024 Aluminum, 3/8" Diameter, 12" Long P/N: 1570K32	\$18.38	1	\$18.38
Wheel	McMaster-Carr – Polyurethane Wheel without Bearing, 5" Diameter x 1-1/4" Wide P/N: 2472T27	\$22.26	1	\$22.26
Bearings for Axle	McMaster-Carr - Ball Bearing, Open, Trade Number R6, for 3/8" Shaft Diameter P/N: 60355K504	\$5.78	2	\$11.56
Shaft Couplings	McMaster-Carr - Two-Piece Shaft Coupling Steel for 1/2" x 3/8" Diameter Keyed Shaft P/N: 60845K53	\$81.41	2	\$162.82
Frame Tubing	McMaster-Carr – General Purpose Aluminum Tubing 1-3/8" OD, 0.049" wall Thickness 89965K411	\$57.67 for 6 feet sections	2	\$115.34
Frame Tube Clamps	Dragon Plate- Carbon Fiber Tube Clamp connects 2.375" and 2.125" tube P/N: FDPCK-TC-250	\$13.50	2	\$27
Attachment	McMaster-Carr- Clamp-on Framing Fitting, Closed Tee Through-Hole Connector for 1" Rail OD	\$3.24	4	\$12.96
Attachment	McMaster-Carr- Steel Ball Knob with 1/4"-20 Threaded Hole, 1/2" Deep	\$4.12	4	\$16.48
Attachment	Need to Manufacture a 1" Aluminum Ball Coupler	\$10.00	4	\$40
Attachment	McMaster-Carr- 6 ft of General-Purpose Aluminum Tubing 1-3/8" OD, 0.049" wall Thickness 89965K411	\$57.67	1	\$57.67
Brakes	Bike Cable Brakes	\$25.05	1	\$25.05

Steering	Custom Hitch Assembly Manufactured from Aluminum	\$50	1	\$50
			Total Price	\$900

Table 15: Redesign Bill of Materials

Chapter 8: Conclusions

Hand rim propulsion wheelchairs can cause upper body injuries and strain. Alternative solutions exist that mitigate muscle strain, but they often use chains which have risks of breakage and derailment. This project created a chainless driven hand cycle wheelchair attachment to combat this shortcoming. The goal was for this device to be easy to use, adjustable, and inexpensive compared to similar products on the market.

The group planned to create a plastic prototype before finalizing a metal arm bike, but due to time restrictions only a plastic prototype was created. The prototype was made from two-inch PVC pipe as the main structure, a nylon rod as the drive shaft, bearings, 3D printed spacers, arm crank, 3D printed gears, bicycle wheel, and the attachment mechanism. The main focus for the prototype was proving the design concept of the drive shaft. Issues and shortcomings with the prototype were material, attachment, and ease of use.

Future plans were devised to convert the prototype into metal and achieve the unmet design parameters. This redesigned arm bike has an estimated total cost of \$900, making it a competitive alternative on the market. The proposed product is an innovative solution that promotes physical activity and diversifies the overall user experience.

Chapter 9: References

- [1] Flemmer, C. L., & Flemmer, R. C. (2015). A review of manual wheelchairs. *Disability and Rehabilitation: Assistive Technology*, 11(3), 177-187. doi:10.3109/17483107.2015.1099747
- [2] Flank, P., Wahman, K., Levi, R., & Fahlström, M. (2012). Prevalence of risk factors for cardiovascular disease stratified by body mass index categories in patients with wheelchair-dependent paraplegia after spinal cord injury. *Journal of Rehabilitation Medicine*, 44(5), 440-443. doi:10.2340/16501977-0964
- [3] Van Der Woude, L., Dallmeijer, A. J., Janssen, T. W., & Veeger, D. (2001). Alternative Modes of Manual Wheelchair Ambulation. *American Journal of Physical Medicine & Rehabilitation*, 80(10), 765-777. doi:10.1097/00002060-200110000-00012
- [4] Whizz-Kidz George. (n.d.). Retrieved March 21, 2019, from <http://www.whizz-kidz.org.uk/meet-the-kidz/george>
- [5] World Health Organization. (2010). Fact Sheet on Wheelchairs. Retrieved January 12, 2019, from http://www.searo.who.int/entity/disabilities_injury_rehabilitation/wheelchair_factsheet.pdf
- [6] Assistive Technology Applications For People With Mobility Impairments. (n.d.). Retrieved January 12, 2019, from http://www.continuetolearn.uiowa.edu/nas1/07c187/Module6/module_6_p6.html
- [7] SpinalCord.com. (2019). Paraplegia. Retrieved January 12, 2019, from <https://www.spinalcord.com/paraplegia>
- [8] Froehlich-Grobe, K., & Lollar, D. (2011, November). Obesity and disability: Time to act. Retrieved from <https://www.ncbi.nlm.nih.gov/pmc/articles/PMC3198028/>
- [9] Wheelchair Facts, Numbers and Figures [Infographic]. (n.d.). Retrieved from <https://kdsmartchair.com/blogs/news/18706123-wheelchair-facts-numbers-and-figures-infographic>
- [10] Types Of Wheelchairs - A Visual Tour. (2019, January 15). Retrieved from <http://www.unitedspinal.org/disability-products-services/types-of-wheelchairs/>
- [11] Louie, E. (2017, April 24). The Parts of a Wheelchair and Its Features. Retrieved from <https://www.karmanhealthcare.com/blog/2017/04/24/the-parts-of-a-wheelchair-and-its-features/>
- [12] Types of Paralysis. (n.d.). Retrieved from <https://www.spinalcord.com/types-of-paralysis>
- [13] Faupin, A., Gorce, P., Watelain, E., Meyer, C., & Thevenon, A. (2010). A Biomechanical Analysis of Handcycling: A Case Study. *Journal of Applied Biomechanics*, 26(2), 240-245. doi:10.1123/jab.26.2.240
- [14] Major Factors and Bio-mechanics. (2012, April 15). Retrieved from <https://jameslacchianaresearch.wordpress.com/2012/04/15/major-factors-and-bio-mechanics-16/>

- [15] Lucas H. V. Van Der Woude, Dallmeijer, A. J., Janssen, T. W., & Veeger, D. (2001). Alternative Modes of Manual Wheelchair Ambulation. *American Journal of Physical Medicine & Rehabilitation*,80(10), 765-777. doi:10.1097/00002060-200110000-00012
- [16] Woude, L. V., Veeger, H., Dallmeijer, A., Janssen, T., & Rozendaal, L. (2001). Biomechanics and physiology in active manual wheelchair propulsion. *Medical Engineering & Physics*,23(10), 713-733. doi:10.1016/s1350-4533(01)00083-2
- [17] L. H. . van der Woude, S. de Groot, and T. W. . Janssen, “Manual wheelchairs: Research and innovation in rehabilitation, sports, daily life and health,” Vol. 28, No. 9, 2006.
- [18] (n.d.). Retrieved from https://www.google.com/imgres?imgurl=http://myplace.frontier.com/~j.schaeff/images/chair8.jpg&imgrefurl=http://myplace.frontier.com/~j.schaeff/index.htm&docid=rFLSTbWGArTILM&tbid=AR8_kJyiKL1MM:&vet=10ahUKEwjI6LqK1MfdAhUBSN8KHSK5Dm4QMwhCKAgwCA..i&w=277&h=213&client=safari&bih=714&biw=1440&q=wheelchair+lever+propulsion+system&ved=0ahUKEwjI6LqK1MfdAhUBSN8KHSK5Dm4QMwhCKAgwCA&iact=mr&uact=8
- [19] U. Arnet, S. V. van Drongelen, der W. van, and H. E. J. Veeger, “Shoulder load during handcycling at different incline and speed conditions,” vol. 27, no. 1, pp. 1–6, 2012
- [20] A. Faupin, P. Gorce, E. Watelain, C. Meyer, and A. Thevenon, “A biomechanical analysis of handcycling: a case study,” Vol. 26, No. 2, pp. 240–245, May 2010.
- [21] Sarraj, A. R., & Massarelli, R. (2011). Design History and Advantages of a New Lever-Propelled Wheelchair Prototype. *International Journal of Advanced Robotic Systems*,8(3), 26. doi:10.5772/10669
- [22] Wijit. (2012). Preservation of Upper Limb Function and the Wijit. Retrieved January 28, 2019, from <http://www.innovationshealth.com/wp-content/uploads/2014/04/Preservation-of-Upper-Limb-Function-and-the-Wijit.pdf>
- [23] Wijit. (2012). *Wijit Driving and Braking System* [Pamphlet]. Roseville, CA: Wijit.
- [24] Baichtal, J., Di Justo, P., Yarbrough, M., Kwityn, J., Roumeliotis, C., Futato, D., Montgomery, K., et al. (2015). *Make : bicycle projects* (First edition.). San Francisco, California: Maker Media.
- [25] Fregly, B. J., Zajac, F. E., & Dairaghi, C. A. (2000). Bicycle Drive System Dynamics: Theory and Experimental Validation. *Journal of Biomechanical Engineering*,122(4), 446. doi:10.1115/1.1286678
- [26] Becker, K. (2018, July 18). This Prototype Chainless Bike May Be The Future of Cycling. Retrieved from <https://www.digitaltrends.com/outdoors/ceramicspeed-chainless-bike-drive/>
- [27] Riomobility. (n.d.). Dragonfly Handcycle User Instruction and Maintenance Manual. Retrieved November 2018, from https://www.rollick.biz/pdf/Dragon_Fly_user_manual.PDF
- [28] Carr. (n.d.). Retrieved from <https://www.mcmaster.com/>

Chapter 10: Appendices

Appendix A: Part Models and Drawings Prototype

Two Inch PVC Pipe

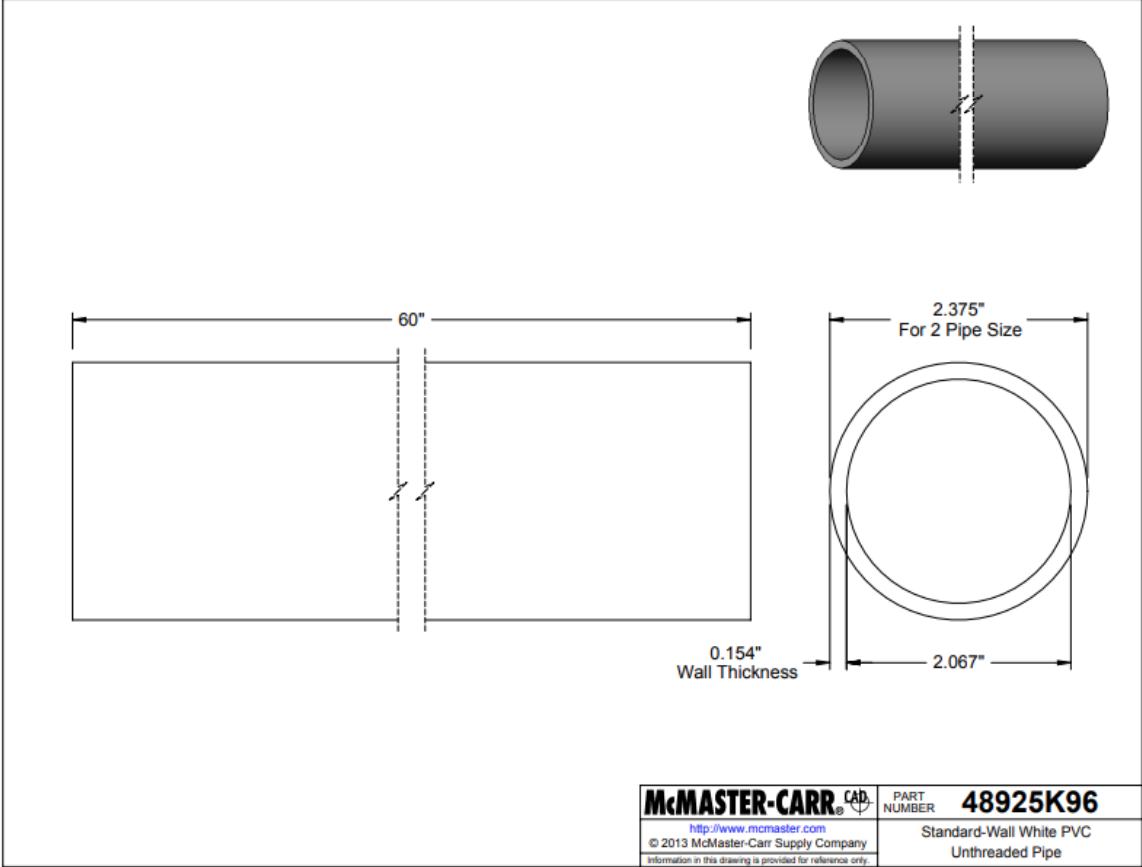


Figure 73: Two Inch PVC Pipe Engineering Drawing [28]

Two Inch Elbow

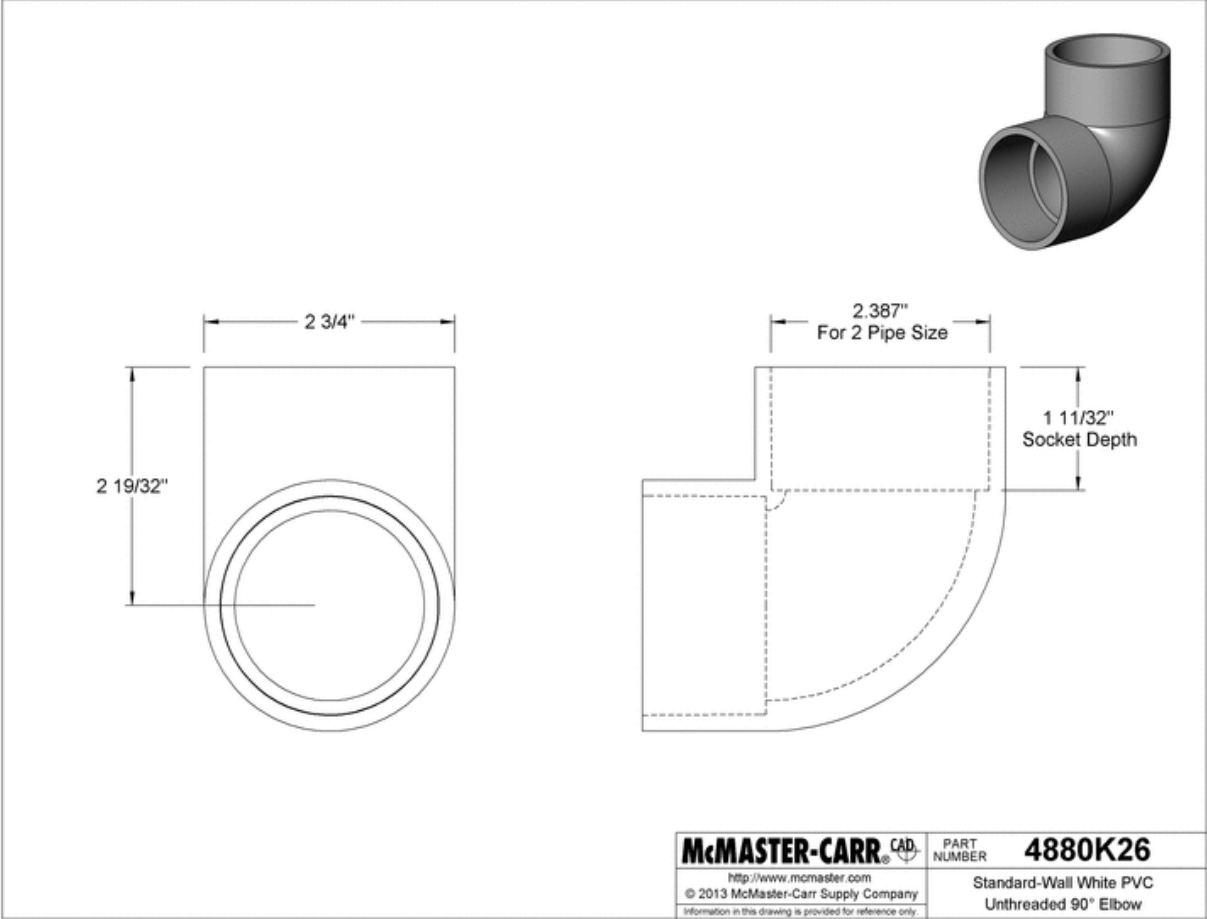


Figure 74: Two Inch PVC Elbow Engineering Drawing [28]

Two Inch T Connector

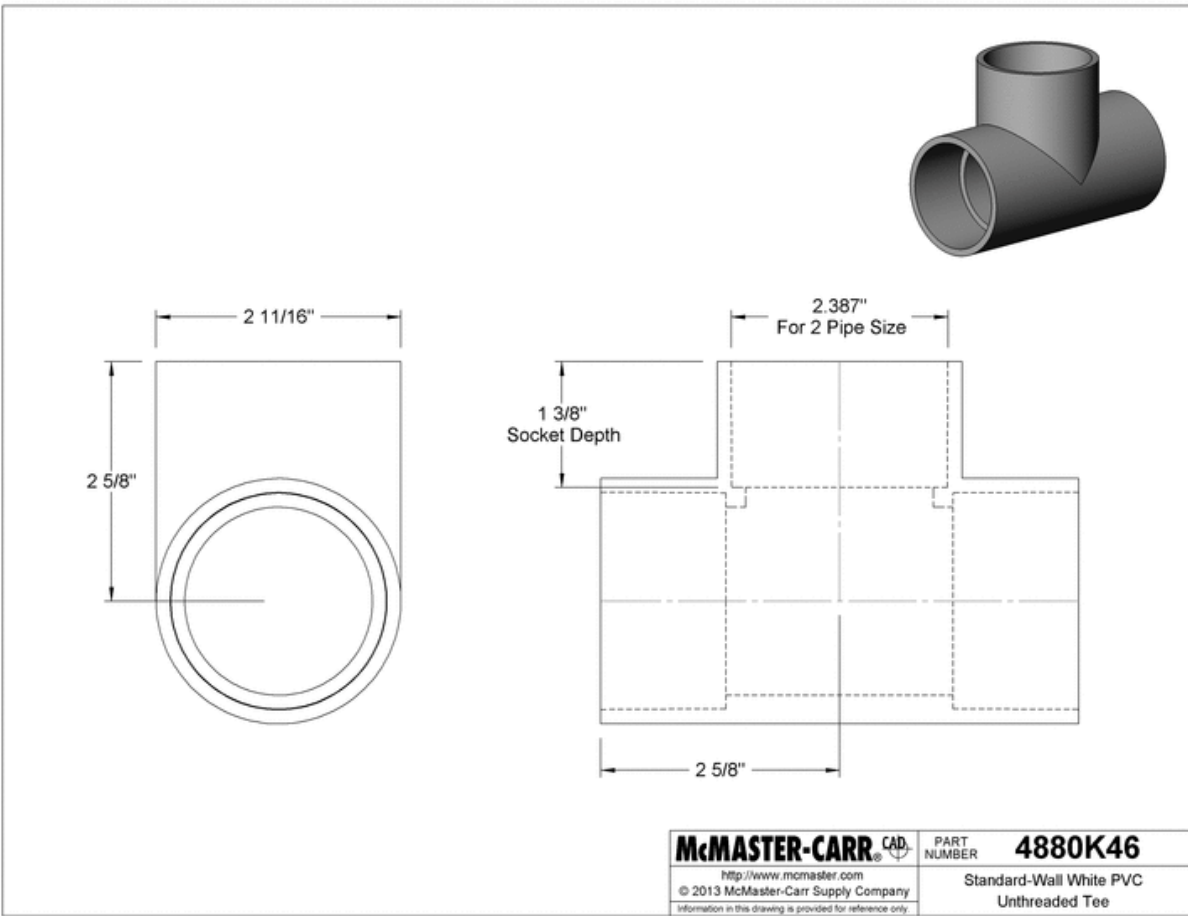


Figure 75: Two Inch PVC Tee Connector Engineering Drawing [28]

3/4 Inch Pipe

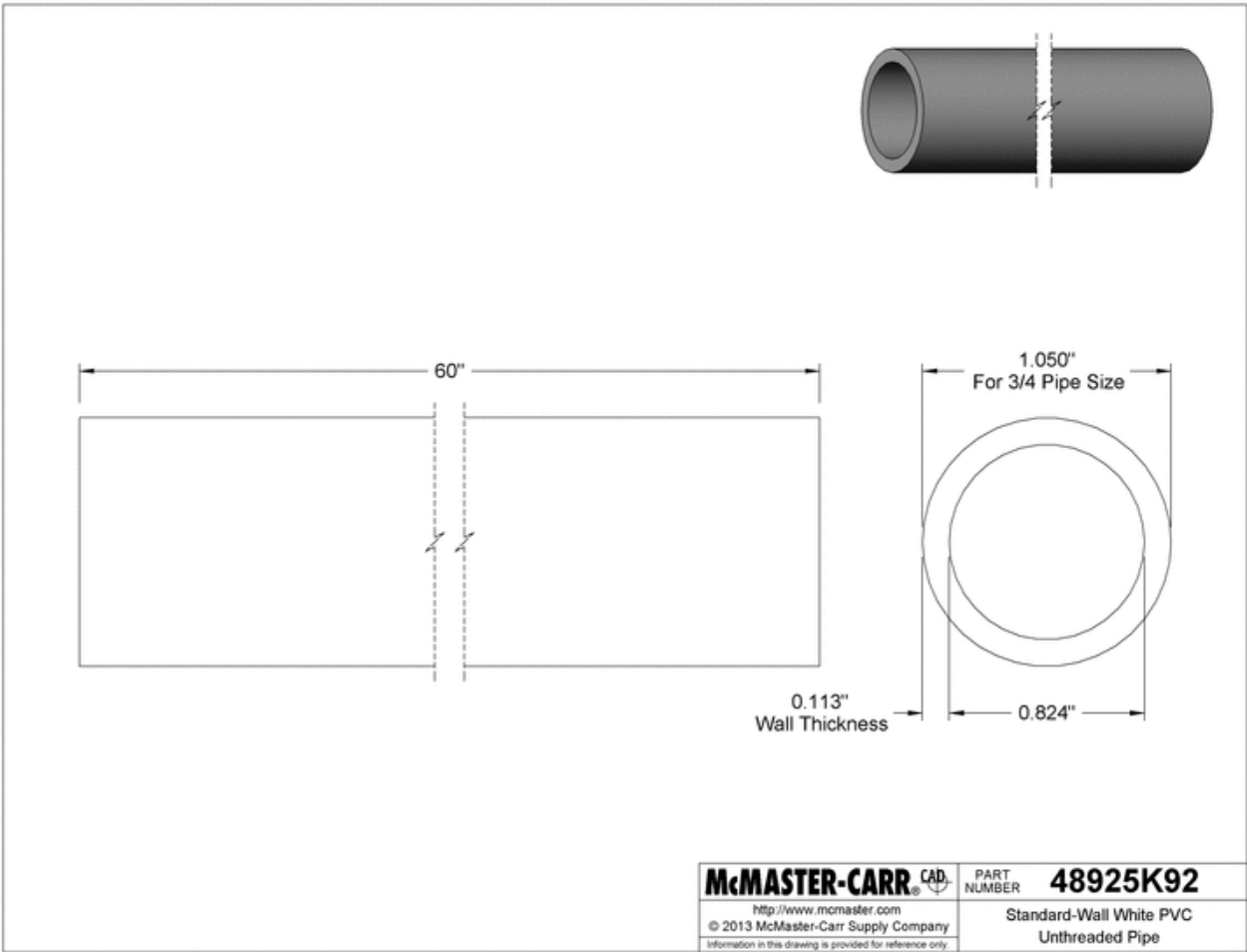


Figure 76: 3/4 Inch PVC Pipe Engineering Drawing [28]

3/4 Inch Elbow

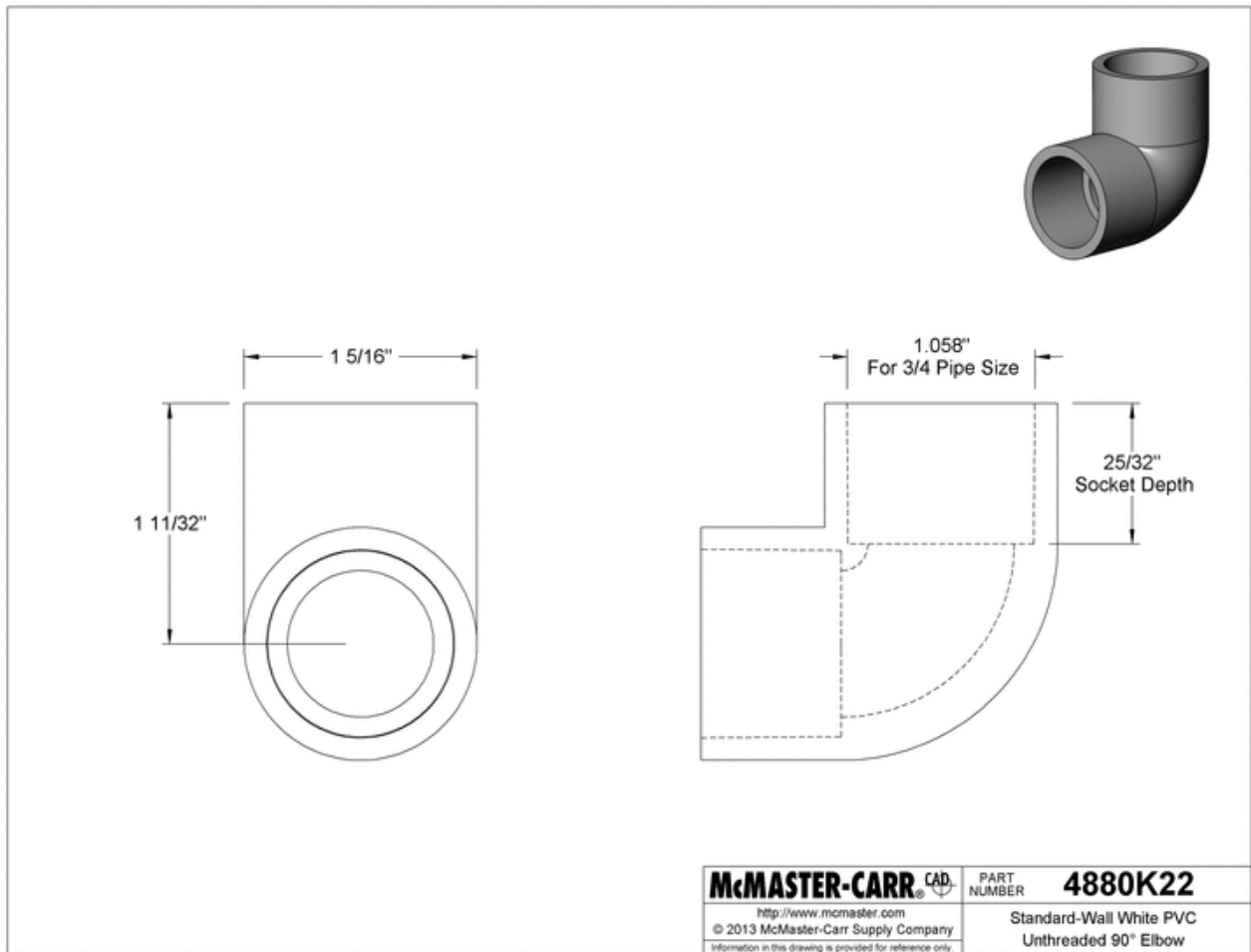


Figure 77: 3/4 Inch PVC Elbow Connector Engineering Drawing [28]

3/4 Inch T Connector

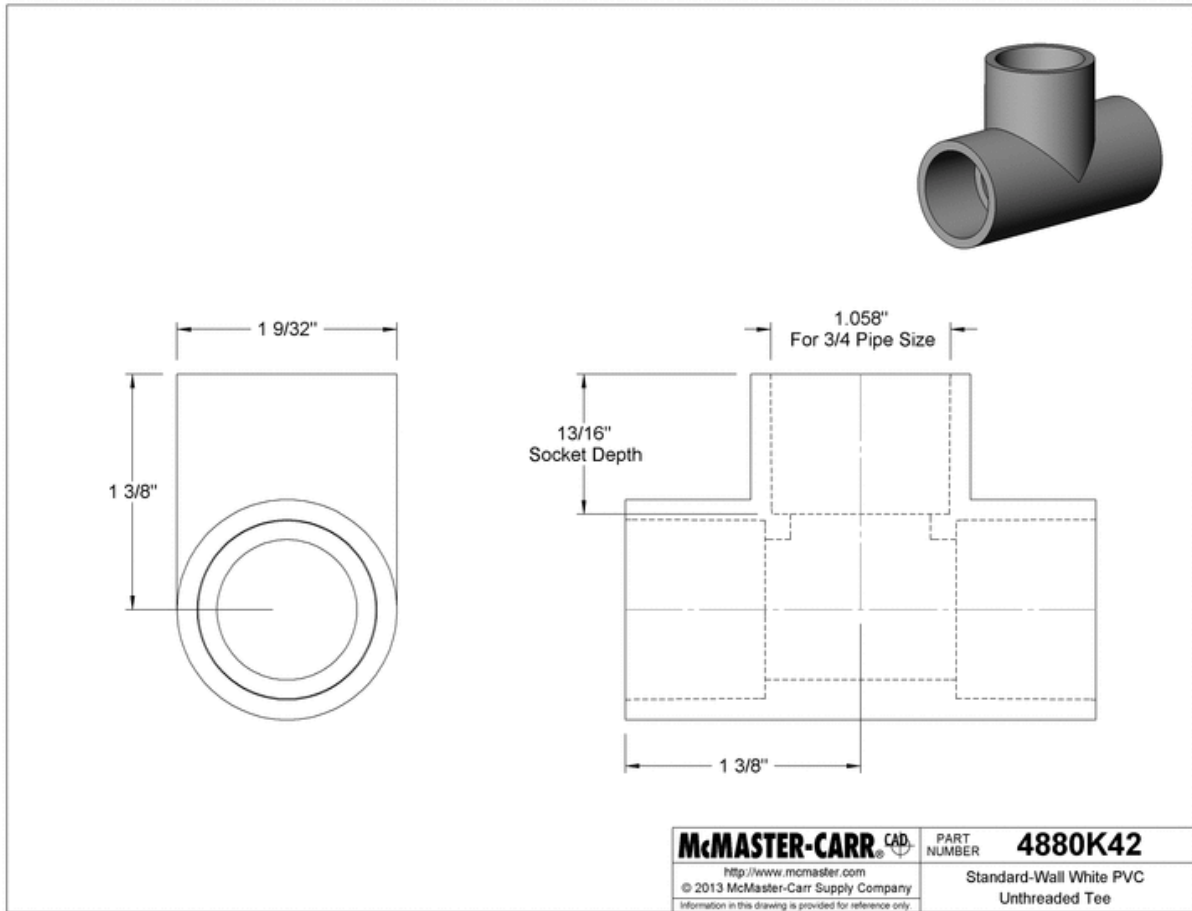


Figure 78: 3/4 Inch PVC Tee Connector Engineering Drawing [28]

3/4 Inch Wye Connector

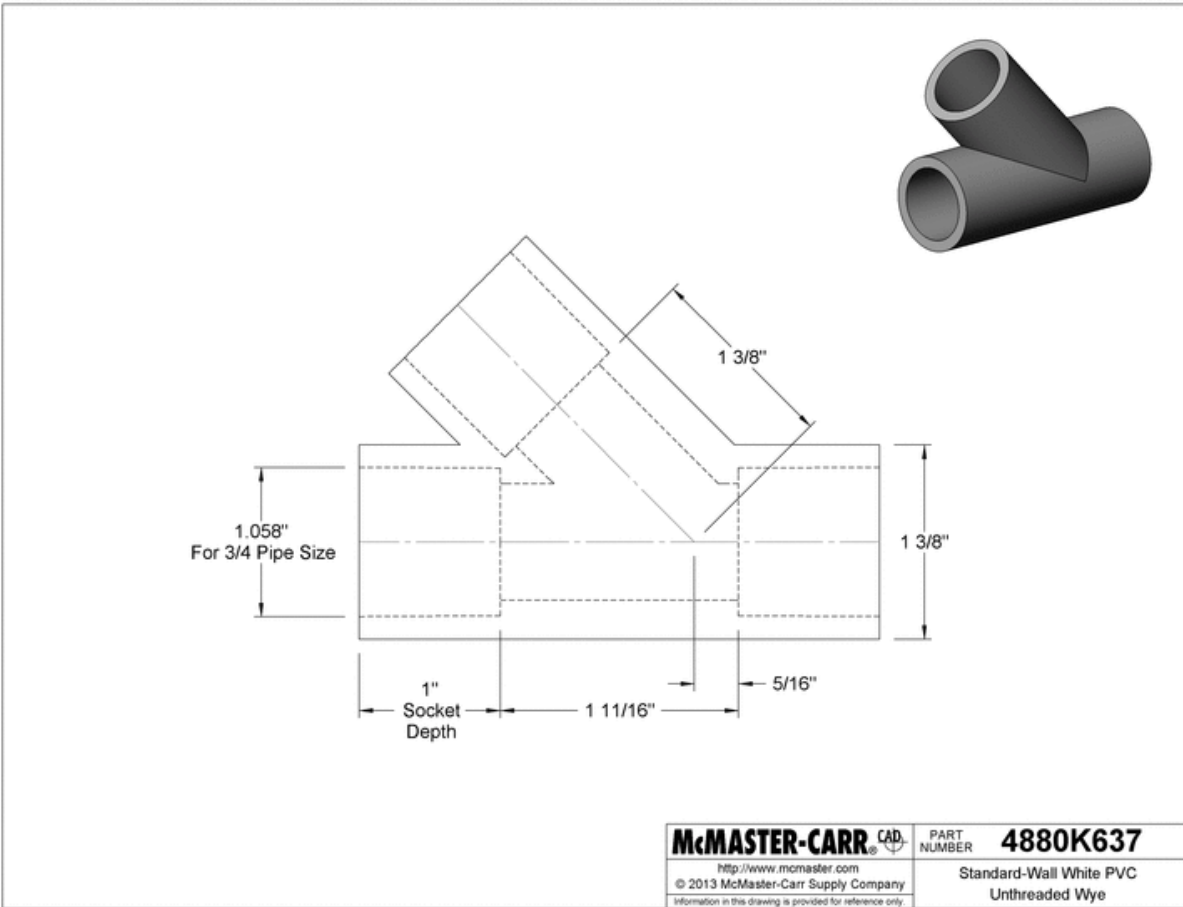


Figure 79: 3/4 Inch PVC Wye Connector Engineering Drawing [28]

Bevel Gear

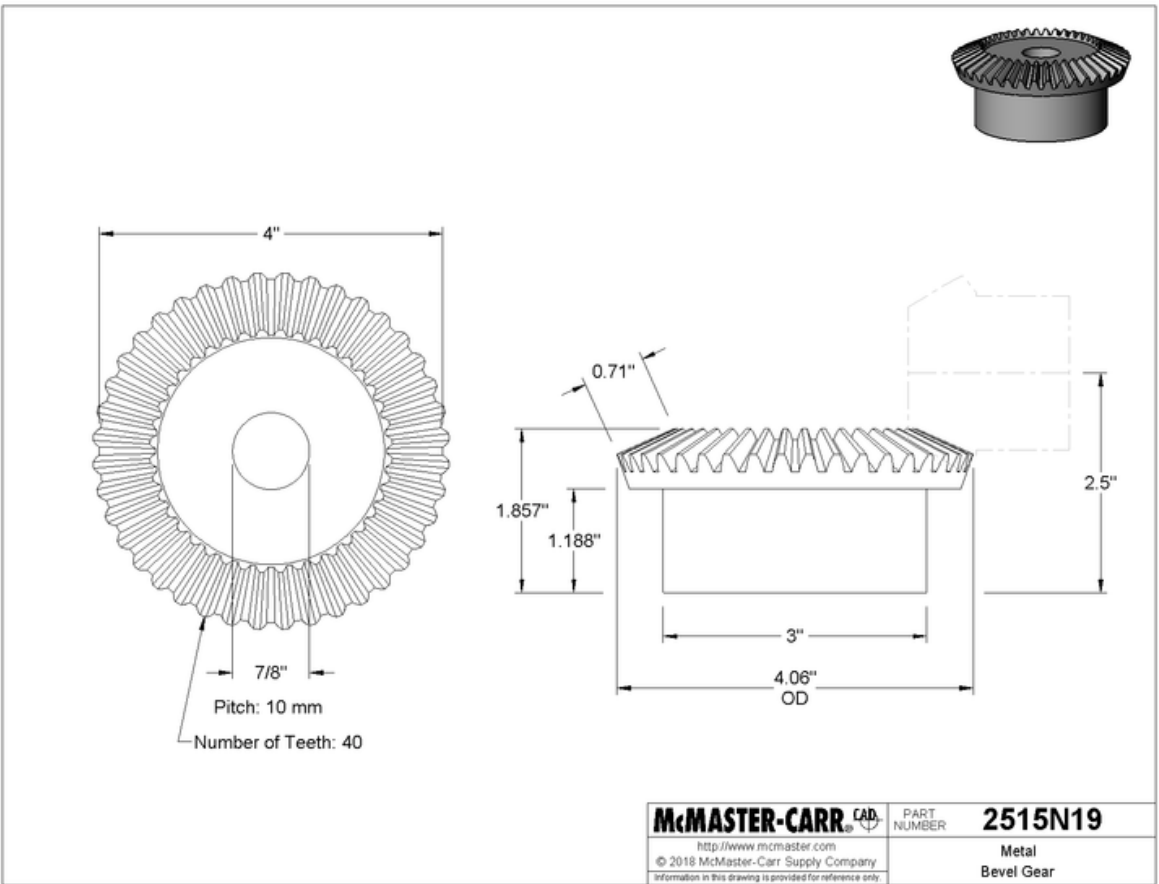


Figure 80: Bevel Gear Engineering Drawing [28]

Bevel Pinion Gear

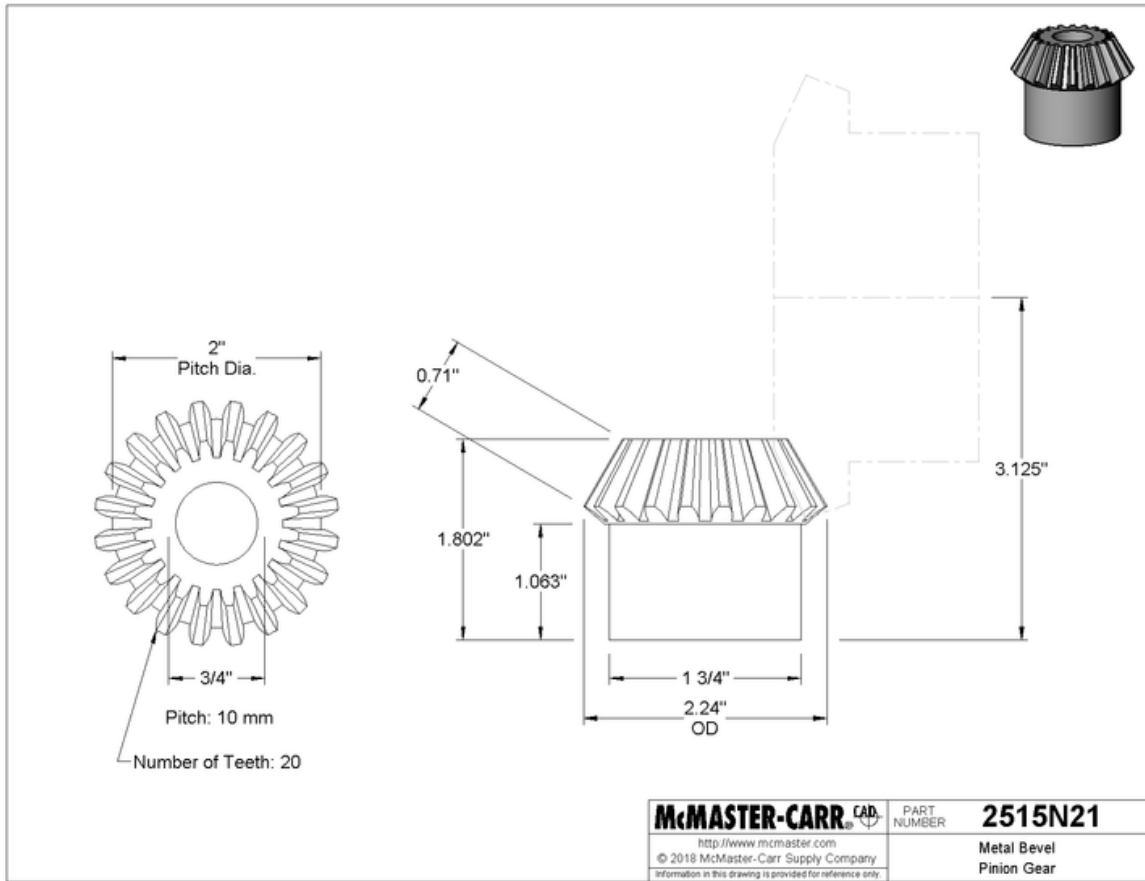


Figure 81: Bevel Pinion Gear Engineering Drawing [28]

Miter Gear

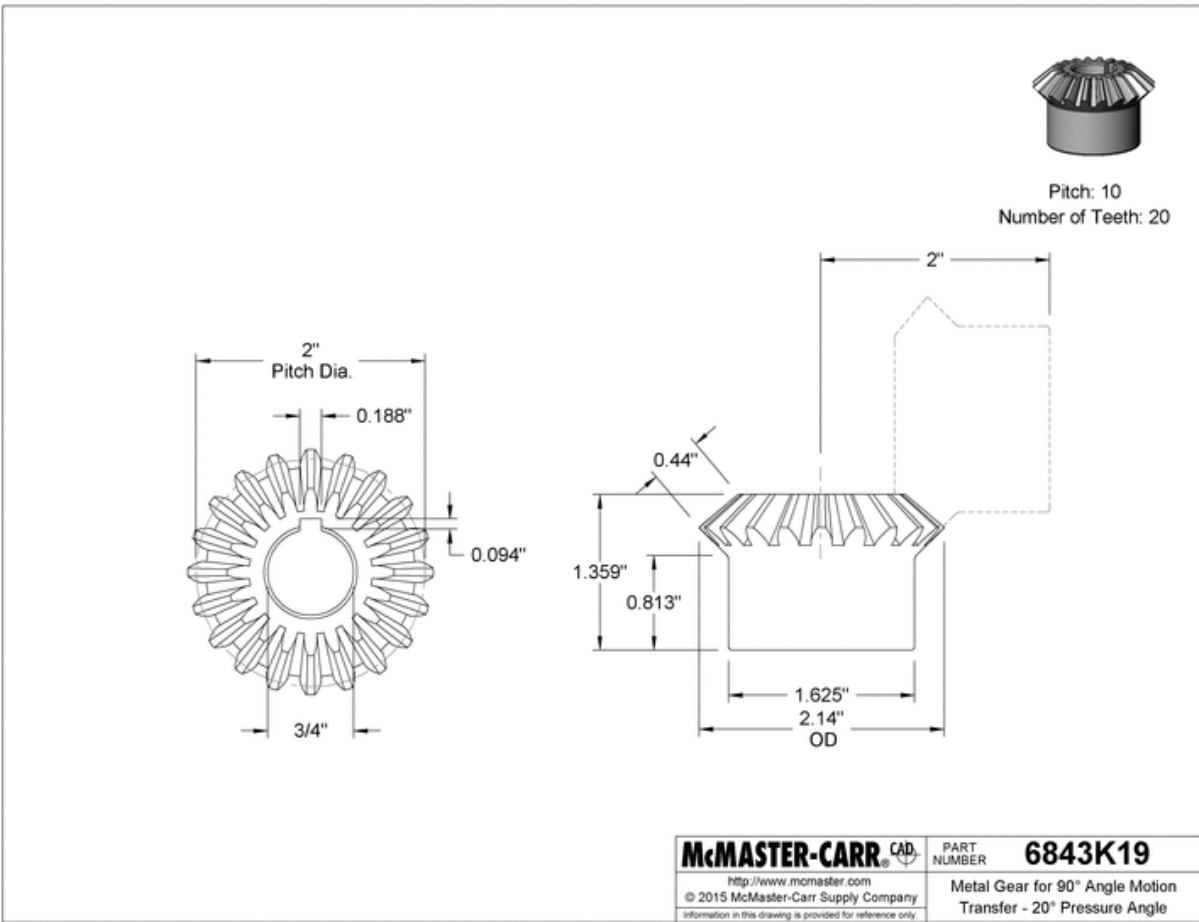


Figure 82: Miter Gear Engineering Drawing [28]

Shoulder Bolt

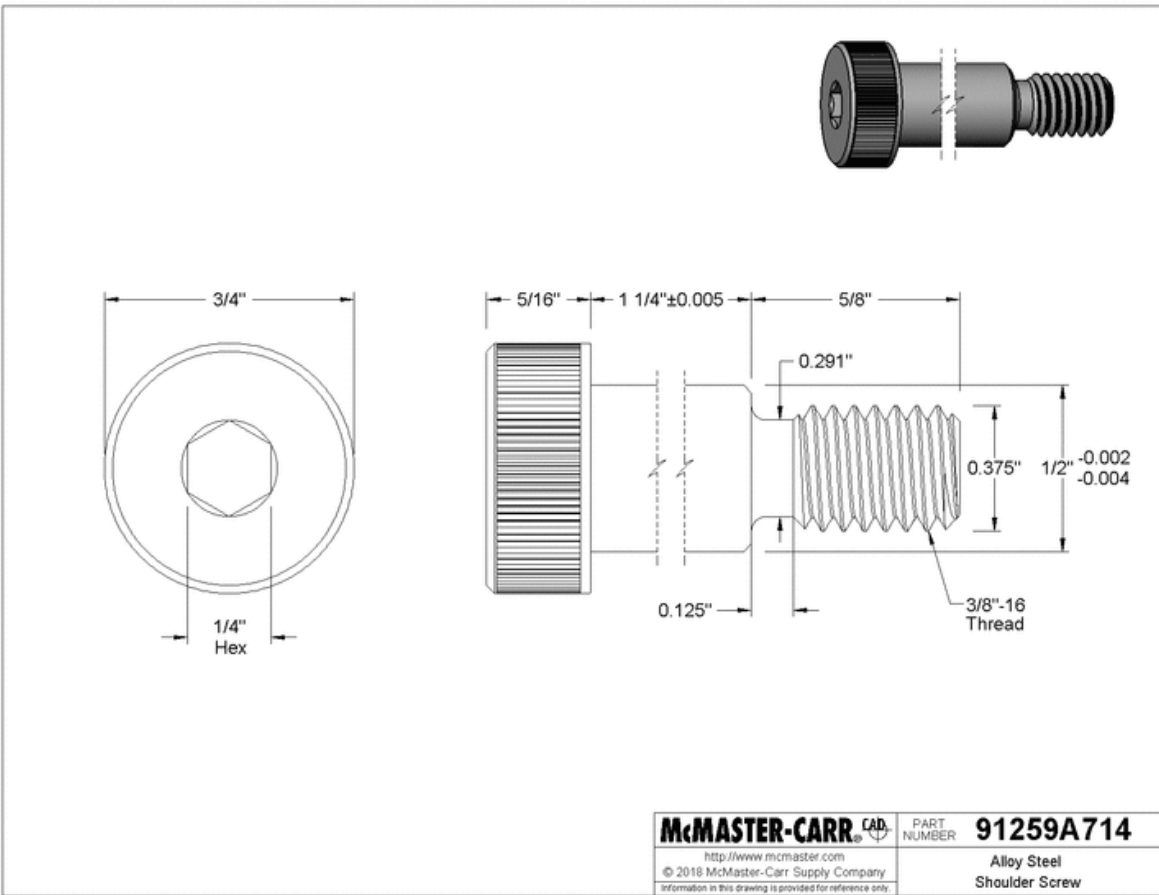


Figure 83: Shoulder Bolt Engineering Drawing [28]

Bearing (Shaft)

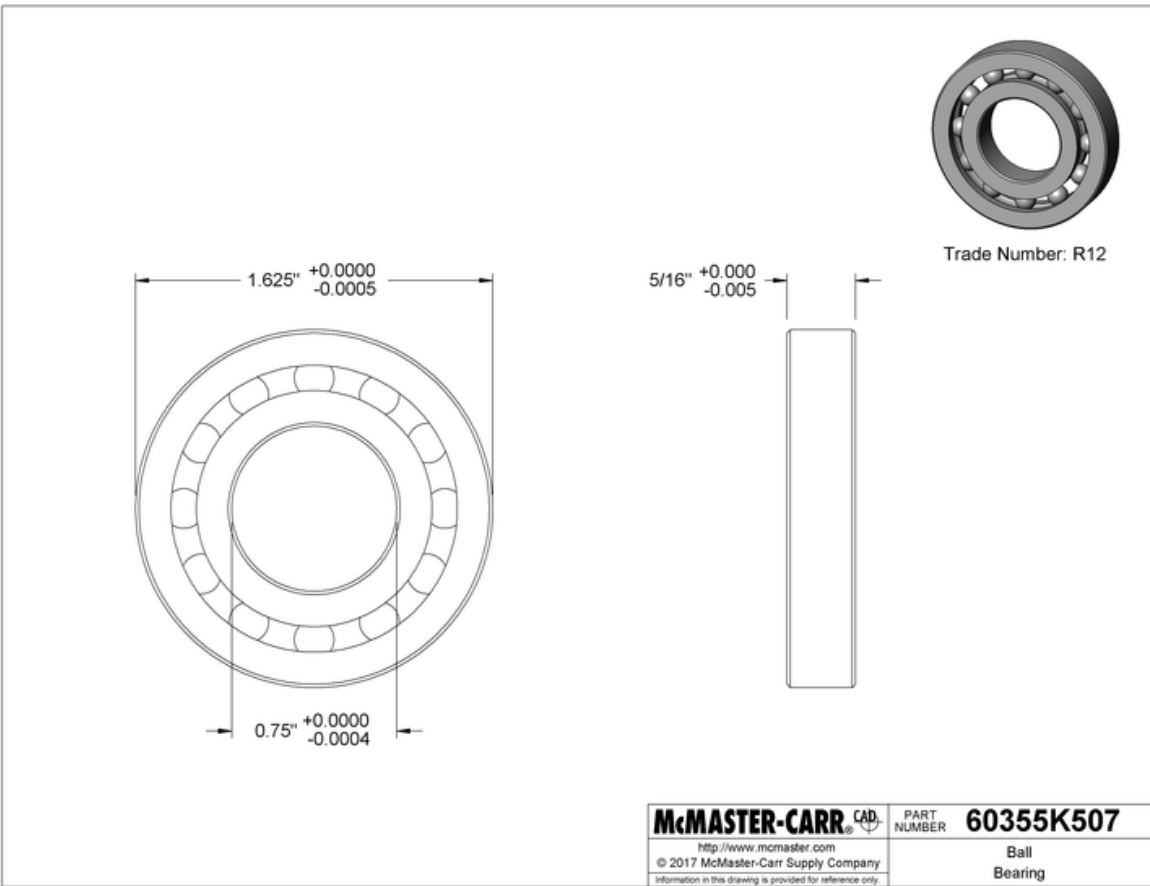


Figure 84: 0.75-Inch Shaft Diameter Ball Bearing Engineering Drawing [28]

Bearing (Axle)

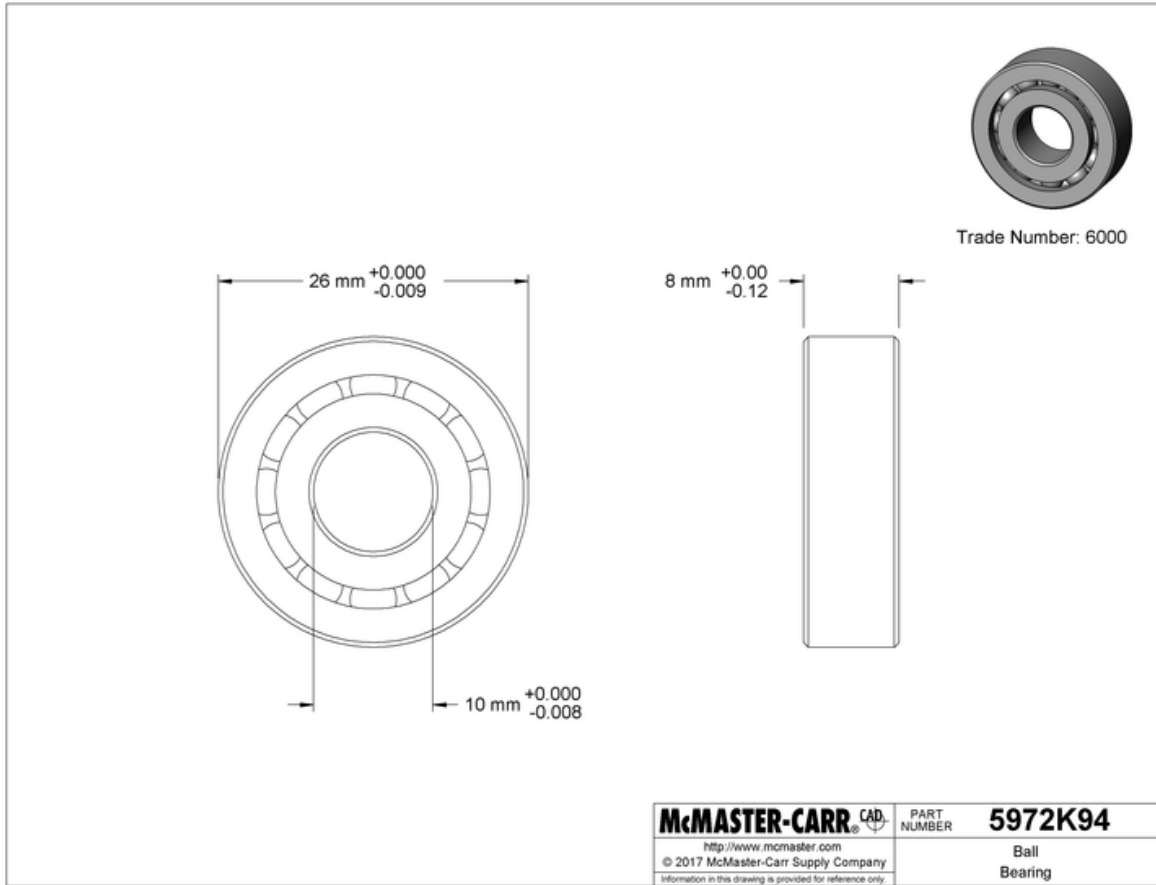


Figure 85: Ten Millimeter Shaft Diameter Ball Bearing Engineering Drawing [28]

Spacer for Fitting (Crank)

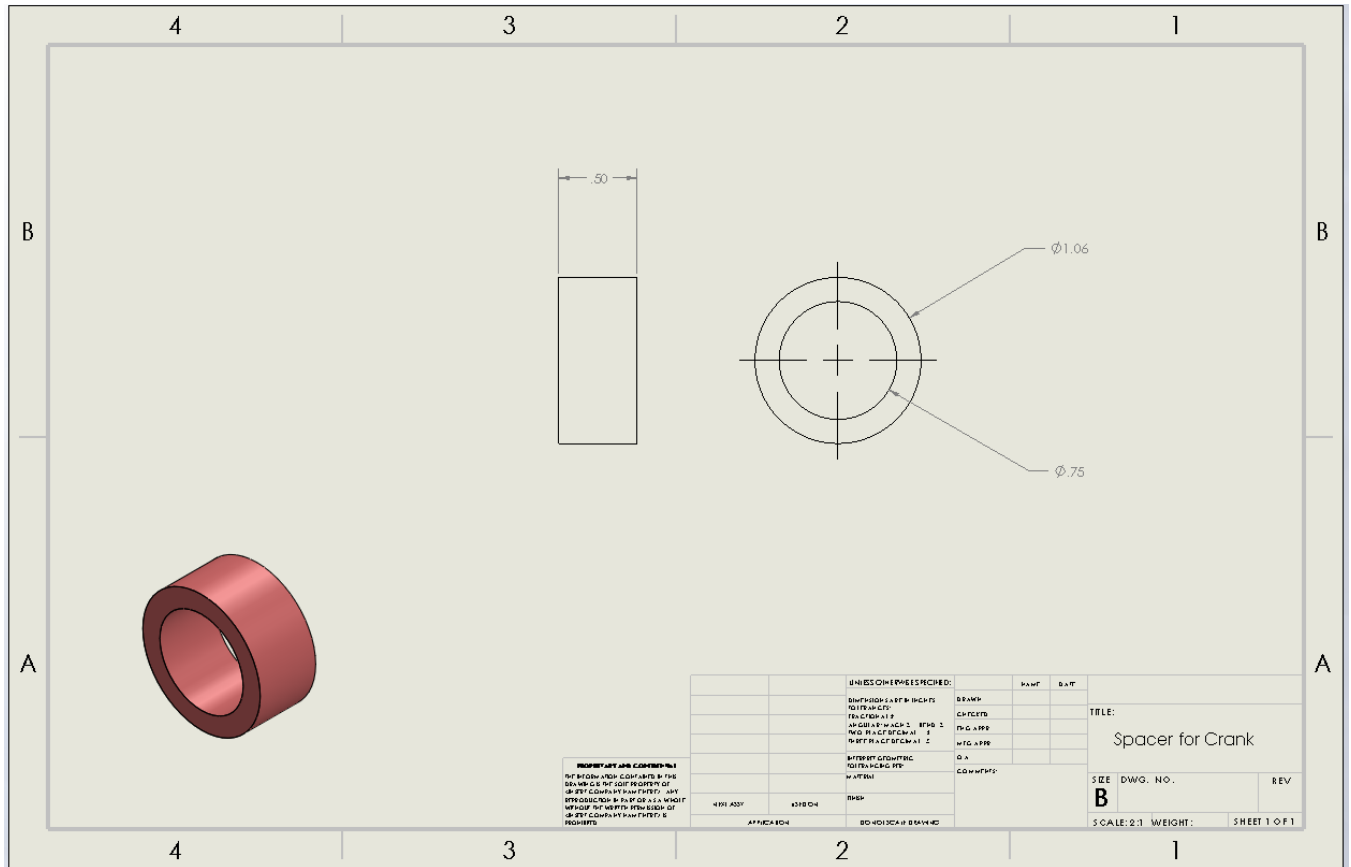


Figure 86: Spacer for Crank Shaft in 3/4-Inch PVC Fitting Engineering Drawing

Spacer for Two-Inch PVC Pipe

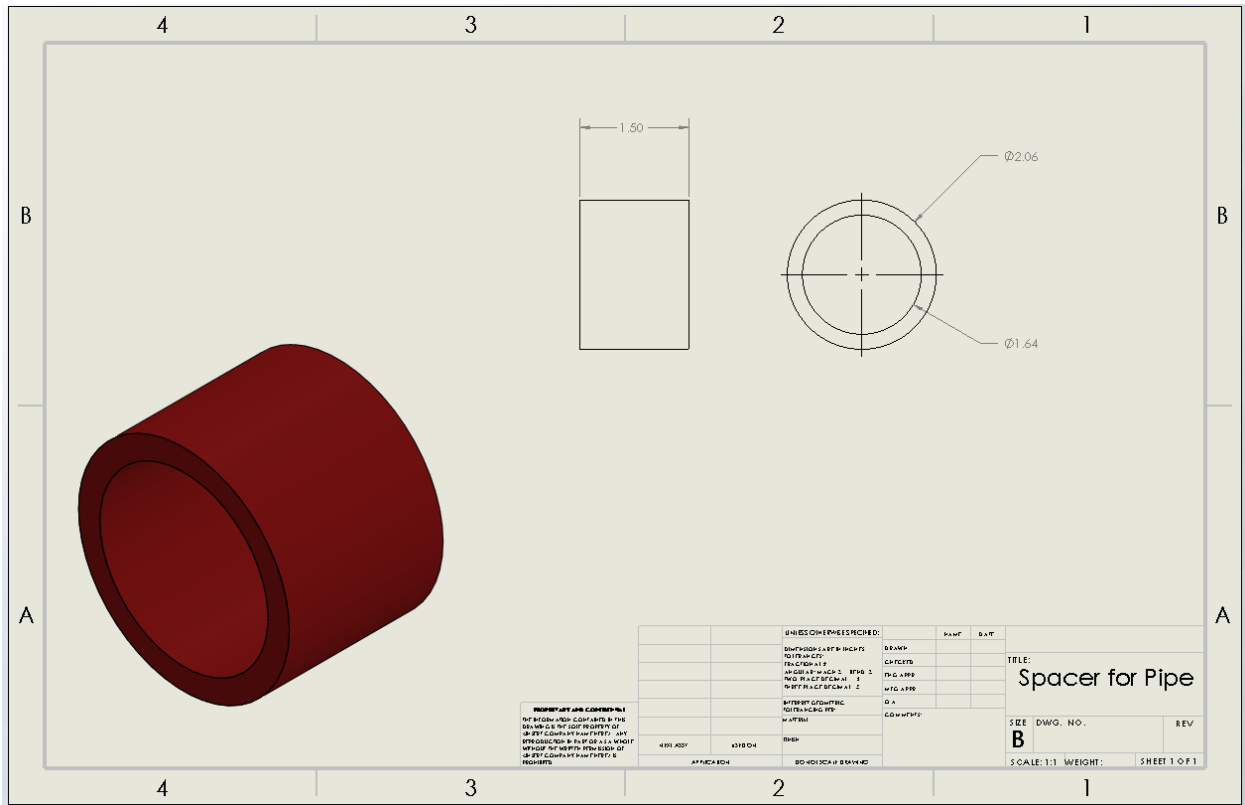


Figure 87: Spacer for Shaft Bearing in Two-Inch PVC Pipe Engineering Drawing

Spacer for Fitting (Shaft)

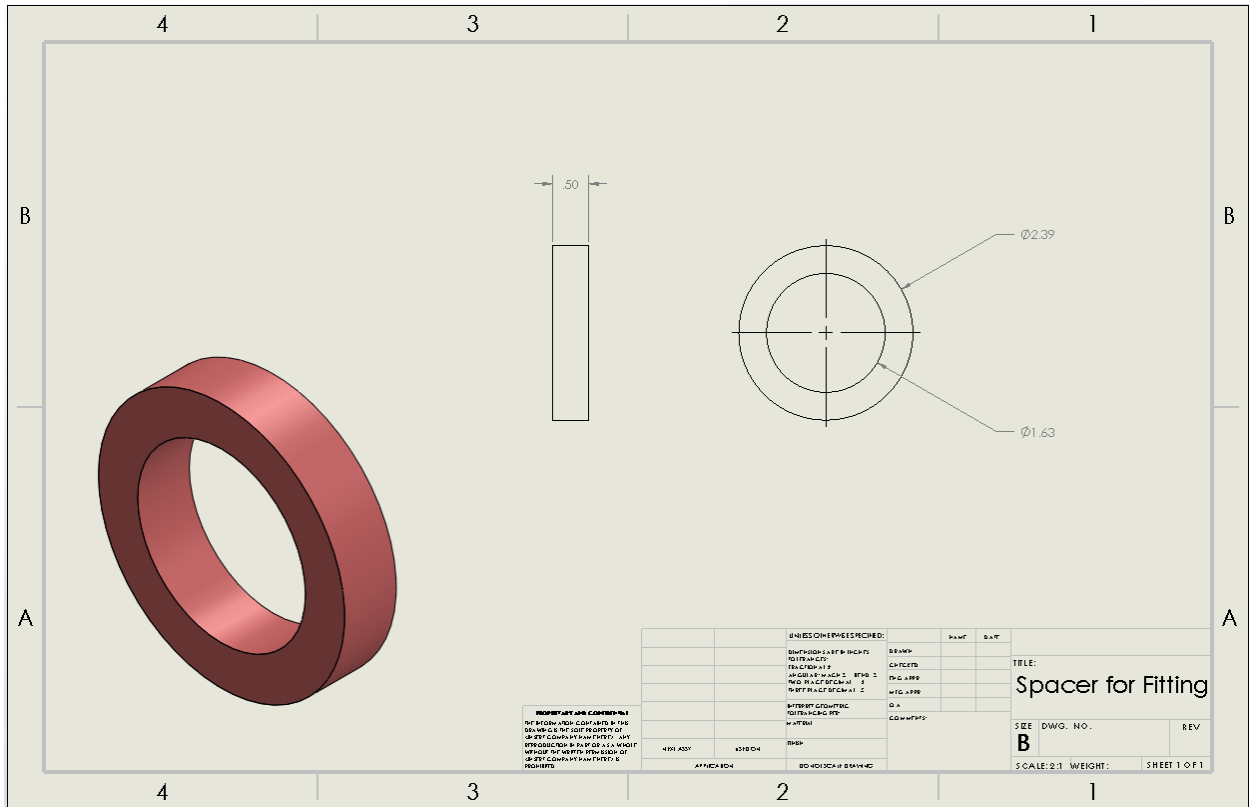


Figure 88: Spacer for Shaft Bearing in Two-Inch PVC Fitting Engineering Drawing

Metal Clip

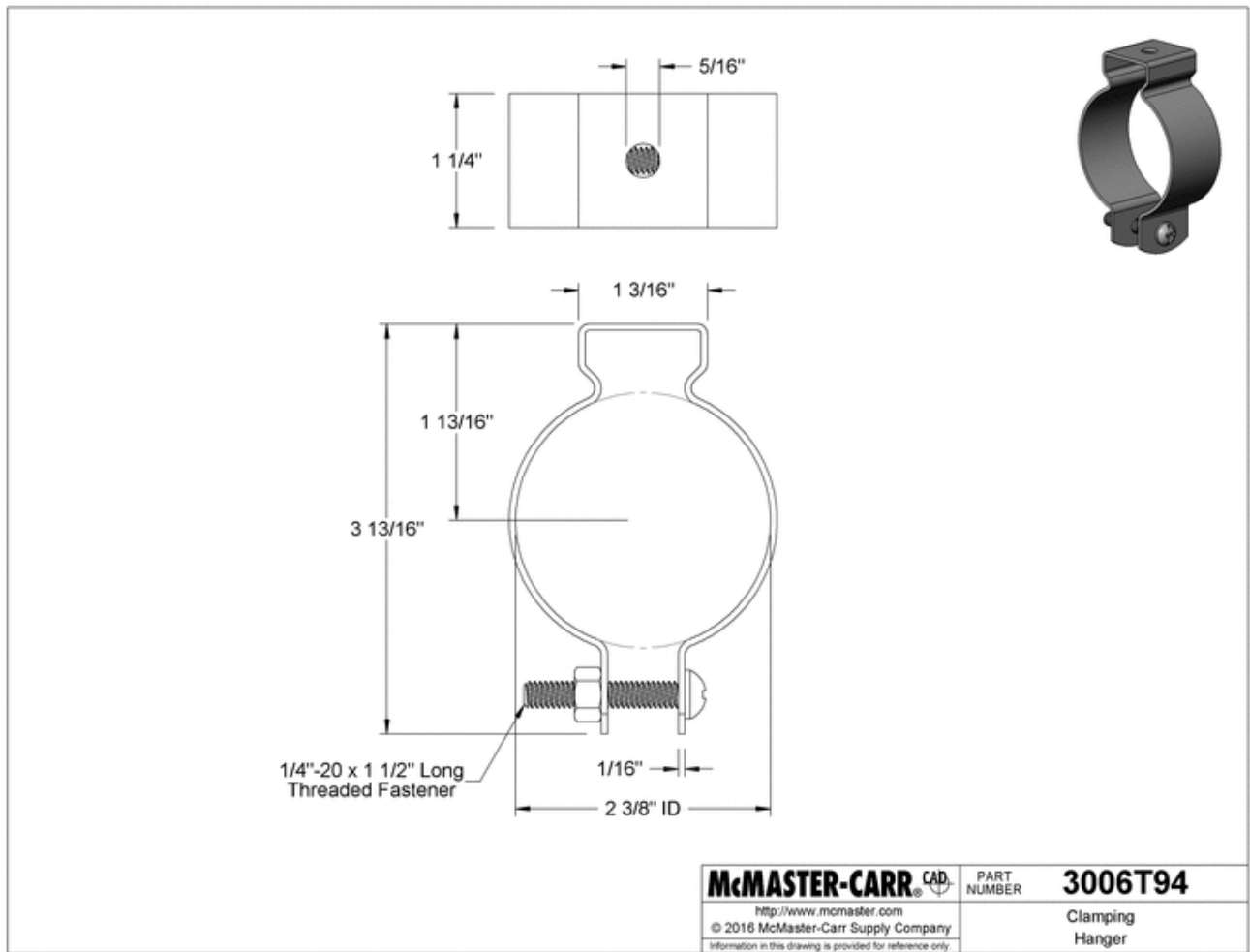


Figure 89: Metal Clip for Attachment Engineering Drawing [28]

Metal Wheelchair Attachment Points

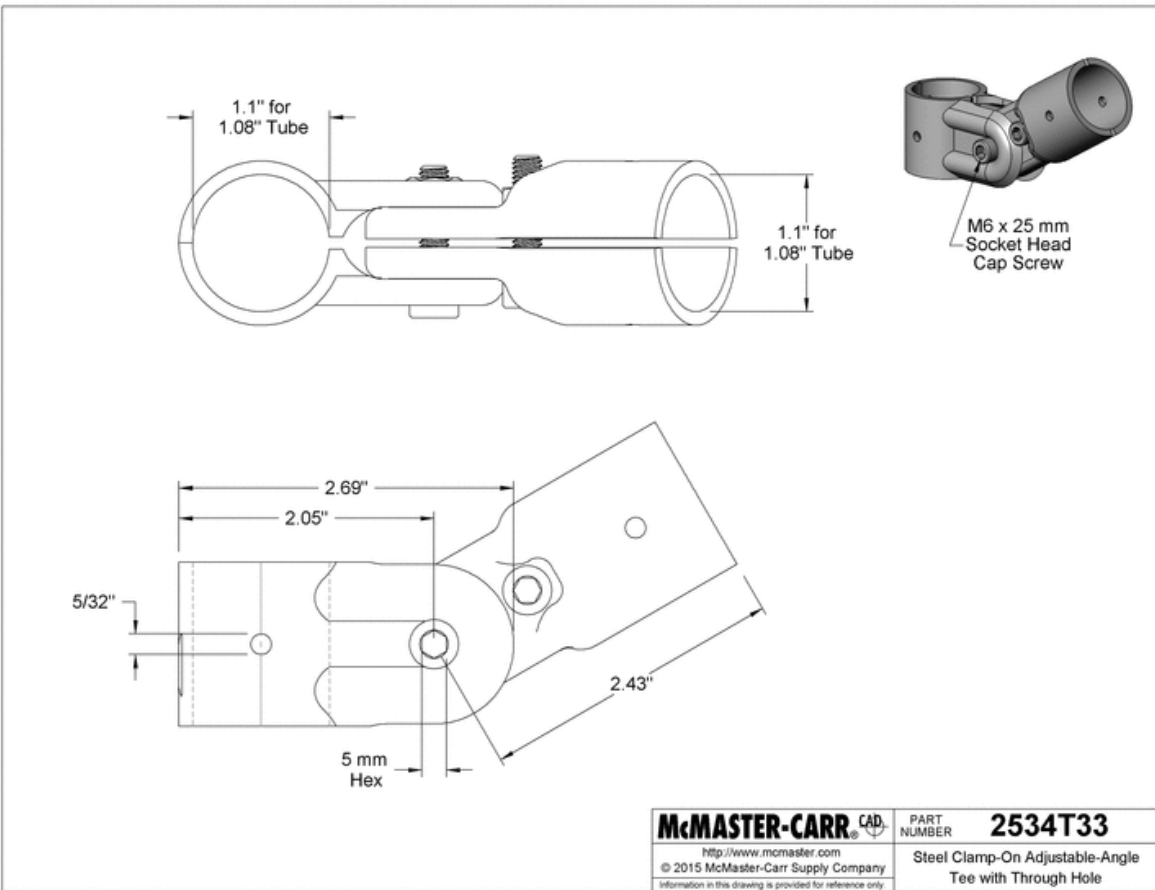


Figure 90: Adjustable Angle Steel Clamp Engineering Drawing [28]

Appendix B: Assembly Drawings Prototype

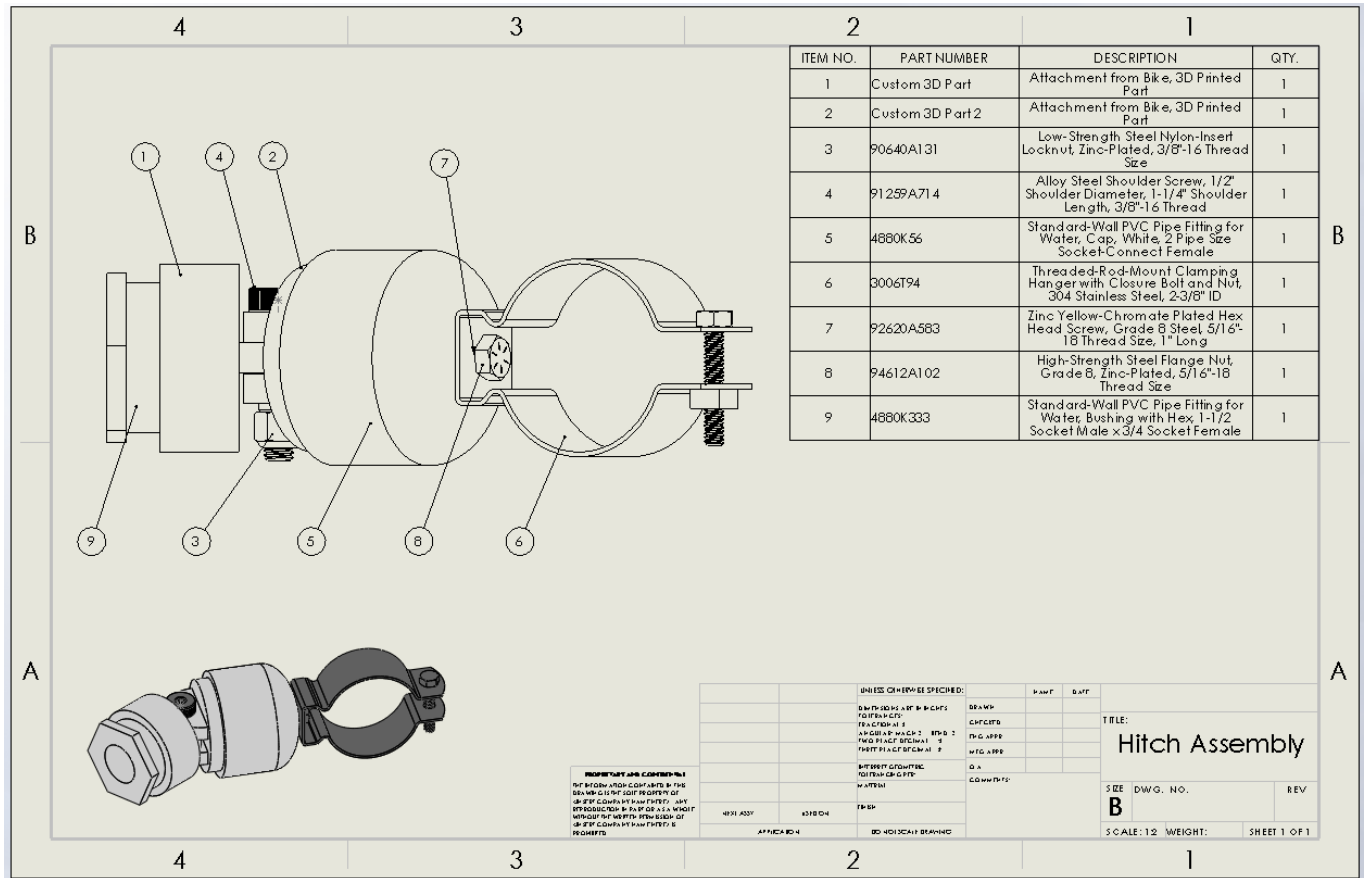


Figure 91: Hitch Assembly Engineering Drawing

Appendix C: Gear Calculations Prototype

Weight of Person	160	lbf	World average weight of adult person	
Weight of Wheelchair	35	lbf		
Weight of Bike	15	lbf		
Total Weight	210	lbf		
Input Force by User	5	lbf	By the ADA Building Standards, door?	
Distance of Force (vertical)	4.22	in	Vertical component of crank subassembly	4.22 in
Moment applied at One Crank Arm	21.1	lbf-in	Force * Distance	
Number of Crank Arms	2			
Total Torque Applied on Crank	42.2	lbf-in	Force and torque is applied at both handles so torque is multiplied	
Number of Teeth of Gear on Crank	20	teeth	Drive	
Number of Teeth of Gear on Shaft	40	teeth	Driven	
Gear Ratio	10		Driven / Drive	
Torque Transmitted to Shaft	422	lbf-in	Torque at gear multiplied by the gear ratio	
Torque Transmitted to Bottom of Shaft	422	lbf-in	The shaft simply transmits torque	
Torque Transmitted to Wheel	422	lbf-in	Miter gear so 1:1 ratio so torque just changes direction	
Radius of Wheel	10	in	Radius of wheel on bike	
Force at Wheel	42.2	lbf	Forward force generated by bike, must be greater than all the other forces; $F = T/D$	

Sum forces to find F_{pull} .
 F_{pull} must be greater than force that is generated at the wheel.

static friction	0.75	static friction coefficient
α	2 degrees	0.034906585 radians
μ	0.004	coefficient of friction - bike tire on asphalt road
g	$\Sigma F_x = ma$	2.2 ft/s ²
	$\Sigma F_y = 0$	

$$F_y : F_{normal} - W_y = 0$$

$$F_y : F_{normal} - W \cos \alpha = 0$$

$$F_{normal} = W \cos \alpha$$

$$F_x : F_{pull} - F_{friction} - W_x = m_{total} a$$

$$F_x : F_{pull} - \mu F_{normal} - W \sin \alpha = m_{total} a$$

$$F_{pull} = m_{total} a + \mu F_{normal} + W \sin \alpha$$

Using above equations solve for F_{pull} , must be less than generated at wheel, F_{pull} represents whats required to move it

F_{normal}	209.872074	lbf
--------------------------------	-------------------	------------

1. assume approach with speed, input 5lbs of force then can make it up the ramp

Using force balance, set $a = 0$ and solve for F_{pull} , this must be less than the force generated at the wheel

8.168382602	using kinetic friction
164.7329496	using static friction

Flat ground, F_{pull}	157.4040553
-------------------------	-------------